Available online at www.sciencedirect.com

SCIENCE DIRECT®

Journal of Volcanology and Geothermal Research 146 (2005) 26–59

Journal of volcanology
and geothermal research

www.elsevier.com/locate/jvolgeores

Anatahan, Northern Mariana Islands: Reconnaissance geological observations during and after the volcanic crisis of spring 1990, and monitoring prior to the May 2003 eruption

Scott K. Rowland[a,*], John P. Lockwood[a,1], Frank A. Trusdell[b], Richard B. Moore[c], Maurice K. Sako[b], Robert Y. Koyanagi[b], George Kojima[b]

[a] *Hawai'i Institute of Geophysics and Planetology, University of Hawai'i at Mānoa, 2525 Correa Rd., Honolulu, HI 96822, USA*
[b] *US Geological Survey Hawaiian Volcano Observatory, P.O. Box 51, Hawai'i Volcanoes National Park, HI 96718, USA*
[c] *US Geological Survey, 520 N. Park Ave., Suite 102, Tucson, AZ 85719, USA*

Received 16 July 2004; accepted 7 October 2004

Abstract

Anatahan island is 9.5 km east–west by 3.5 km north–south and truncated by an elongate caldera 5 km east–west by 2.5 km north–south. A steep-walled pit crater ~1 km across and ~200 m deep occupies the eastern part of the caldera. The island is the summit region of a mostly submarine stratovolcano. The oldest subaerial rocks (stage 1) are exposed low on the outer flanks and in the caldera walls. These include thick (~10 m) and thin (2–3 m) lava flows, well-indurated tuffs, and scoria units that make up the bulk of the island. Rock compositions range from basaltic andesite to dacite, and most are plagioclase-phyric. On the steep north and south flanks of the volcano, these rocks are cut by numerous east–west-oriented, few-hundred-m-long lineaments of undetermined origin. Indurated breccias unconformably overlie scarps cut into stage 1 units low on the south flank. Intermediate-age eruptive units (stage 2) include caldera-filling lava flows and pyroclastic deposits and, on the outer flanks, vents and valley-filling lava flows. The youngest pre-2003 volcanic unit on Anatahan (stage 3) is a hydromagmatic surge and fall deposit rich in accretionary lapilli. Prior to 2003, this unit was found over almost the entire island, and in many places original depositional surfaces and outcrops could be found in high-energy environments along the coast, indicating a young (but undetermined) age. During reconnaissance visits in 1990, 1992, 1994, and 2001, geothermal activity (fumaroles as well as pits with boiling, sediment-laden pools) was observed in the southern part of the pit crater.

In March and April 1990, increased local seismicity, a large regional earthquake, and reported increased fumarolic activity in the pit crater prompted evacuation of Anatahan village, at the west end of the island. Our first field investigation took place in late April 1990 to assess the level of volcanic unrest, conduct reconnaissance geological observations, collect rock and geothermal water samples, and set up a geophysical monitoring network. Results at this time were inconclusive with

---

[*] Corresponding author. Tel.: +1 808 956 3150; fax: +1 808 956 5512.
E-mail address: scott@hawaii.edu (S.K. Rowland).

[1] Present address: Geohazards Consultants International Inc., P.O. Box 479, Volcano, HI 96785, USA.

0377-0273/$ - see front matter © 2005 Elsevier B.V. All rights reserved.
doi:10.1016/j.jvolgeores.2004.10.020

respect to determining whether the activity was anomalous. Water in some of the geothermal pits within the pit crater was boiling, and pH values as low as 0.7 were recorded in the field. An electronic distance measurement (EDM) network was installed, and over a ~1-week period, up to 9 cm of extension occurred across some lines but not others. Seismicity was characterized by intermittent local earthquakes but no sustained swarms or tremor. A brief visit in June 1990 revealed that the shallow lake near the boiling pits was gone, but activity in the pits themselves was similar to that of April 1990. Only minor extension had occurred along a single EDM line since the previous visit, and no earthquakes >M2.5 occurred during the visit.

Subsequent 1- to 2-day visits occurred in October 1990, May 1992, May 1994, and June 2001. Activity within the geothermal pits was relatively constant during every visit, although during this 11-year period the level of the water in each pit decreased. In June 2001, a ~50-m-wide region of mud pots and steaming ground in the central part of the geothermal area had developed. No geologic evidence, however, suggested that an eruption would occur <2 years afterward. Most of the EDM lines showed slight extension between late 1990 and 1992, followed by very gradual contraction from 1992 to 2001. A more extensive seismic-monitoring system was installed on the Northern Mariana Islands during these visits, and it recorded a small seismic swarm at Anatahan from May to July 1993. The telemetry component of the seismic equipment broke prior to 2001 and had not been repaired by the time of the May 2003 eruption, so no precursory seismic data were recorded to indicate pre-eruption unrest.

© 2005 Elsevier B.V. All rights reserved.

Keywords: Anatahan; Mariana; caldera; geothermal; stratovolcano; EDM

1. Introduction

The Mariana archipelago consists of a frontal island arc to the east and an active magmatic arc to the west (Fig. 1). The frontal arc consists of numerous seamounts and undersea platforms as well as four large islands (Guam, Rota, Tinian, and Saipan) that consist of uplifted limestone overlying Eocene volcanic rocks (e.g. Cloud et al., 1956; Karig, 1971). The active arc includes 12 islands and banks plus numerous seamounts extending ~1700 km north–south along a line concave to the west. Anatahan is located in the southern half of the magmatic arc (Fig. 1). The Mariana Islands form a relatively typical intra-oceanic volcanic arc and result from volcanism and uplift associated with westward subduction of the Pacific Plate under the Philippine Sea Plate (e.g. Bloomer et al., 1989; Fryer, 1996; Stern et al., 2003). Politically, Guam is a territory of the United States, whereas all the other Mariana islands comprise the Commonwealth of the Northern Mariana Islands (CNMI), tied loosely to the USA.

Recorded volcanic activity along the magmatic arc extends from Esmeralda Bank, ~25 km southwest of Tinian, to Uracas (also called Farallon de Pajaros; Fig. 1). Esmeralda Bank reaches to within ~40 m of the ocean surface and sulfurous seawater is often reported at this location (Corwin, 1971; Gorshkov et al., 1982; Bloomer et al., 1989; Simkin and Siebert, 1994). Eruptions have been recorded at 12 subaerial and submarine volcanoes of the magmatic arc (Table 1). The most recent was that of Anatahan, starting in May of 2003 and continuing as of this writing (April 2005). Many of the islands are visited infrequently, and small eruptions could have gone unreported, particularly prior to the 1950s.

Anatahan, centered at 16°21′N, 145°40′E, is a little more than 100 km north of Saipan and can sometimes be seen from there on a clear day. Anatahan showed unrest in the spring of 1990, starting with a seismic crisis in March and April (BGVN, 1990a,b,c). The authors and others were members of a volcanic crisis response team sent to the island initially in April 1990 to assess the situation at the request of the CNMI government (Koyanagi et al., 1990; BGVN, 1990b) and then later for follow-on studies. These return visits, to continue geological observations and geophysical measurements as well as to install permanent seismometers, occurred in June 1990 (Sako et al., 1990; BGVN, 1990c), October 1990 (BGVN, 1990d,e; Moore et al., 1991), May 1992 (BGVN, 1992; Moore et al., 1993), May 1994 (Sako et al., 1995), and June 2001 (Trusdell et al., 2001). Completion of this long-

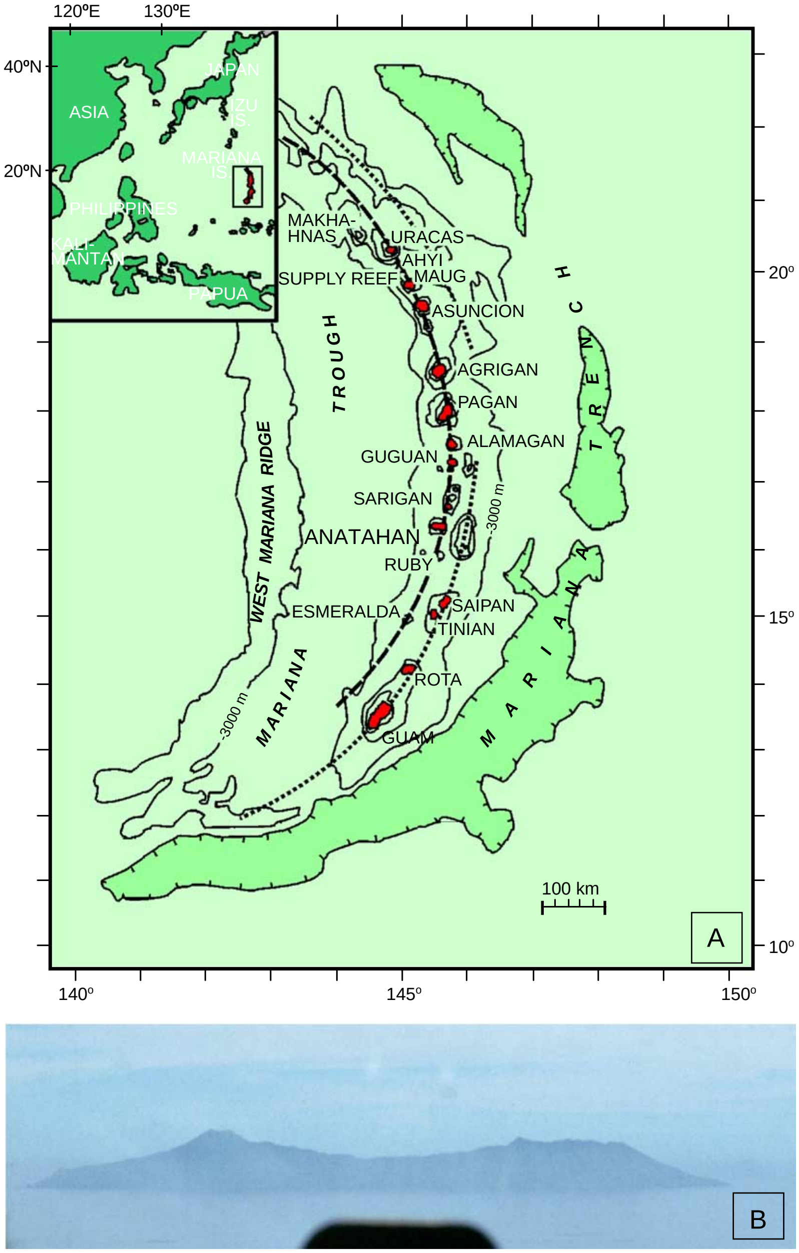
120ºE
130ºE
40ºN
20ºN
ASIA
JAPAN
IZU IS.
MARIANA IS.
PHILIPPINES
KALI-MANTAN
PAPUA
MAKHA-HNAS
URACAS
AHYI
SUPPLY REEF
MAUG
ASUNCION
AGRIGAN
PAGAN
ALAMAGAN
GUGUAN
SARIGAN
ANATAHAN
RUBY
ESMERALDA
SAIPAN
TINIAN
ROTA
GUAM
TROUGH
WEST MARIANA RIDGE
MARIANA
-3000 m
-3000 m
MARIANA TRENCH
100 km
20º
15º
10º
140º
145º
150º
A
B

Fig. 1. A) Location map of the Mariana Islands (adapted from Karig, 1971). *Dashed* and *dotted* lines indicate active magmatic and frontal arcs, respectively. Generalized bathymetric contours are at 1000 m intervals, and *gray shading* indicates water depths >6000 m. B) Anatahan viewed from due south while approaching by helicopter. The lowest point on the skyline is the lowest point on the southern caldera rim.

delayed report was prompted by the eruption that commenced in May 2003 (BGVN, 2003a,b,c,d,e, 2004; Trusdell et al., 2005-this issue). We hope that the information presented here will provide a basis for understanding and visualizing this most recent activity. Our results are based on observations from the ground, boats, helicopters, and stereo airphotos, and from geophysical measurements.

2. Previous geological investigations

Other than entries in catalogs of world volcanoes (e.g. Kuno, 1962; Simkin and Siebert, 1994), almost no geological information has been published about Anatahan. Tanakadate (1940) presents a topographic map very similar to the modern version (Fig. 2) and reports a hot spring along the southern coastline. Meijer et al. (1983) report radiometric ages of 1.31 ± 0.21 and 0.40 ± 0.11 million years for flows on the northeast and northwest coastlines. These locations, as we note below, correspond to the oldest stage of our generalized stratigraphy.

3. General morphology

Anatahan is an elongate stratovolcano truncated by an elongate caldera (Fig. 2). It is merely the subaerial portion of a large volcanic construct that is radially symmetric below sea level and rises ~2500 m from the surrounding sea floor (Chadwick et al., 2005-this issue). The east–west dimension of the island (9.5 km) is nearly 3 times the north–south dimension (3.5 km), and its subaerial area is ~30 km^2. The outer flanks of the volcano are cut by numerous gullies and valleys and have average slopes of ~30°. However, slopes are not consistent around the island; much of the northern flank has average slopes of ~35°, whereas the western flank slopes average ~25°. The northern flank is the most heavily vegetated and deeply gullied part of the island.

Table 1
Recorded eruptions in the Mariana Islands

Volcano	Eruption dates	References
Esmeralda Bank	1944, 1964, 1970, 1975, 1982, 1987	1, 2, 3
Ruby	1966, 1995	3, 4, 5
Anatahan	2003 to present (June 2004)	6, 7, 8, 9, 10, 11
Guguan	1883	3, 12
Alamagan	1864(?), 1887(?)	3, 12, 13, 14, 15
S. Pagan	1864, 1929(?)	3
N. Pagan	1669, 1825, 1873, 1909, 1917, 1923, 1925, 1981, 1982, 1987, 1988, 1992, 1993	3, 16, 17, 18
Asuncion	1690(?), 1775(?), 1906, 1924(?)	3, 12
Supply Reef	1969, 1985(?), 1989	3, 19
Ahyi	1979(?), 2001	3, 19
Makhahnas	1967	19
Uracas (Farallon de Pajaros)	1864, 1874(?), 1900(?), 1912, 1925, 1928, 1932, 1934, 1936, 1939, 1941, 1943, 1947, 1951, 1952, 1967	3, 12

[1] SEAN (1987); [2] McClelland et al. (1989); [3] Simkin and Siebert (1994); [4] BGVN (1995); [5] Norris and Johnson (1969); [6] BGVN (2003a); [7] BGVN (2003b); [8] BGVN (2003c); [9] BGVN (2003d); [10] BGVN (2003e); [11] BGVN (2004); [12] BGVN (1992); [13] BGVN (1990d); [14] BGVN (1999); [15] Moore and Trusdell (1993); [16] Banks et al. (1984); [17] Koyanagi et al. (1993); [18] BGVN (1994); [19] BGVN (2001).

The highest point on the island (790 m) is immediately west of the caldera. Flank slopes are essentially radial to this location, and it may have also been a topographic high prior to caldera formation. Other local topographic highs occur around the rim of the caldera, the highest reaching almost 700 m along the northeast rim. Both the island and the caldera are narrowest at their centers, and, combined with the two highest points essentially at either end of the caldera, give the impression that the island is composed of two coalesced volcanic edifices (Fig. 1B; Tanakadate, 1940). The caldera clearly consists of multiple collapse structures (see below), but our limited sampling and mapping did not resolve whether two edifices exist. Bathymetric data (Chadwick et al., 2005-this issue) strongly suggest that Anatahan is a single volcano. Most of the island is thickly vegetated by tall grasses and closely packed shrubs and trees, which combined with the steep slopes, make overland travel difficult (Maruyama, 1954).

4. The caldera

The caldera is ~10 km^2 in size and occupies approximately a third of the island's area. Its east–west dimension is ~5 km, approximately twice its shortest north–south dimension (~2.5 km). The caldera rim is lowest to the north and south and highest to the east and west (Fig. 2). In some locations (e.g. to the north) the inner walls are nearly vertical, whereas elsewhere (e.g. to the south) they slope from rim to floor at less than 20°. The caldera can be subdivided into west and east portions occupying 2/3 and 1/3 of the caldera area, respectively. Together, they give the caldera a vague

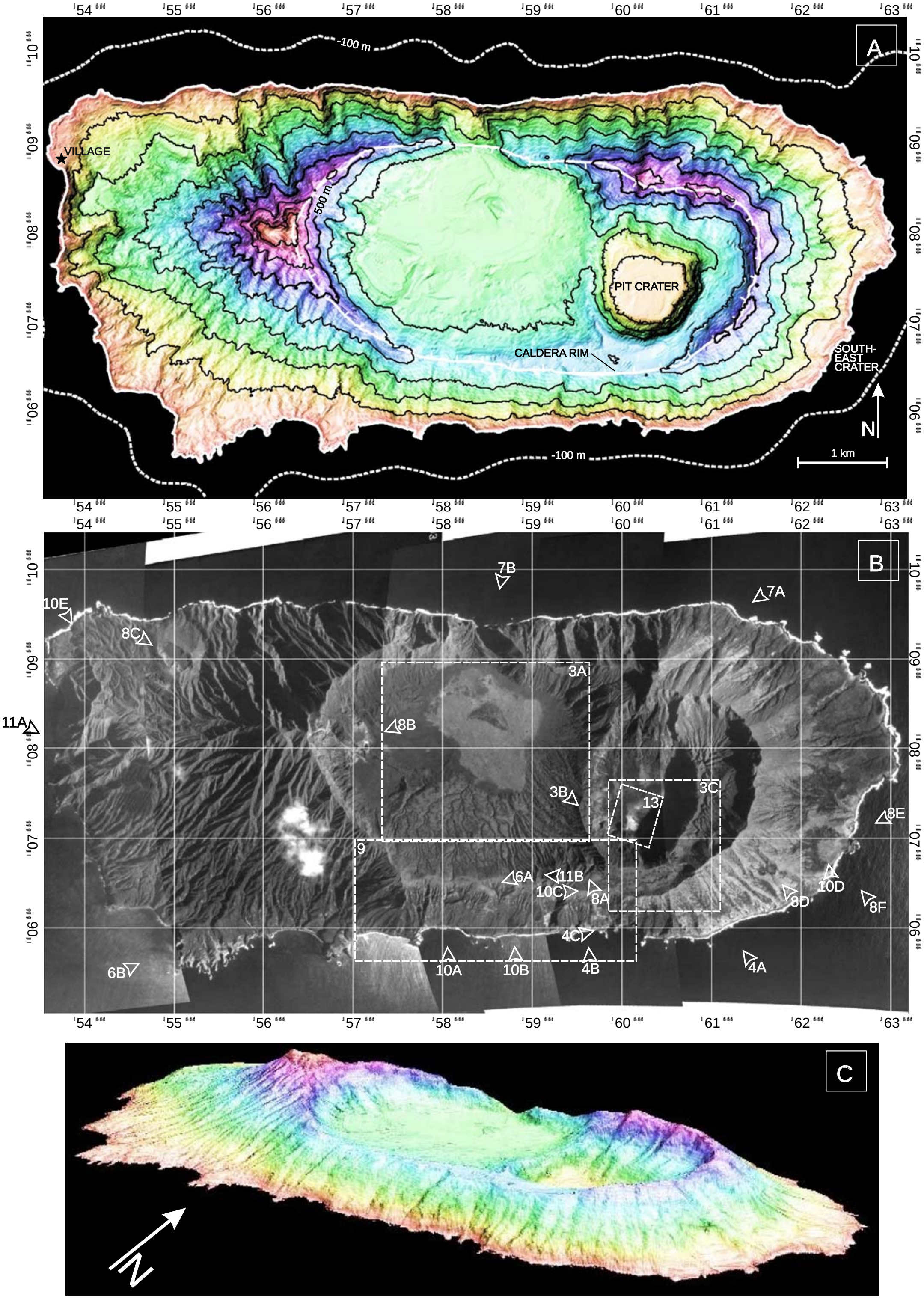
A
-100 m
VILLAGE
500 m
PIT CRATER
CALDERA RIM
SOUTH-EAST CRATER
N
1 km
-100 m
54
55
56
57
58
59
60
61
62
63
10
09
08
07
06
B
7B
7A
10E
8C
3A
11A
8B
3B
3C
13
8E
9
6A
11B
10C
8A
10D
8D
8F
4C
10A
10B
4B
4A
6B
C
N

∞ shape, suggesting that the caldera formed from the coalescence of two closely spaced collapse structures. The northern and western floor of the west portion acts as a sediment sink for material washing in from the south and east as well as off the caldera walls. This nearly horizontal floor is mostly covered with light-toned grass (Fig. 2B) and is interrupted by at least five partially buried scoria or ash rings (Fig. 3A).

The southwestern to eastern parts of the west caldera portion consist of a gently sloping ramp of gullied pyroclastic material. To the southwest, south, and southeast, this ramp extends to the caldera rim; to the east, it extends to the rim of the pit crater (see below). The gullies to the southwest and south are separated by planar interfluves, whereas those to the southeast and east are separated by ridges. A relatively distinct boundary separates these areas of differing gully density (Fig. 3A). The downslope edge of this ramp is truncated by a ~10 m-high curvilinear scarp, which can be extended to include the remnant of a pyroclastic cone (Fig. 3A).

The eastern portion of the caldera is occupied almost entirely by a steep-walled pit crater ~1 km across and ~200 m deep. The east, south, and west walls of this pit crater are the steepest, averaging ~50°. Exposed in the pit crater walls are multiple layered deposits that appear from a distance to be relatively horizontal and laterally extensive (Fig. 3B). Prior to the 2003 eruption, the pit crater floor, with an area of approximately 0.5 km^2, sloped gently southward. In the southern part of the pit crater, geothermal activity consisting of boiling muddy water in small pits (sometimes submerged in a shallow lake), occurred. At the base of the southeastern wall was a fuming area of sulfur accumulation.

The southern part of the pit crater appears to have been the site of geothermal activity for at least the past few decades. Air photographs taken in 1944 and 1952 (Fig. 3C) show essentially this same location to be partially devoid of vegetation and hydrothermally altered (suggested by light-toned ground), although the unvegetated area is smaller than that between 1990 and 2001. Additionally, the map of Maruyama (1954), drawn during or shortly after World War II, shows a steaming "volcanic crater" roughly in the southeast part of the caldera.

5. Flank lava flows and volcaniclastic units

On the north and south flanks are lava flows and volcaniclastic units that compose the bulk of Anatahan (Fig. 4). They are exposed along the wave-cut cliffs just above a narrow coastal shelf, in erosional gullies that extend upslope almost to the caldera rim, as well as in the caldera walls. They are the oldest rocks of the volcano, grouped into stage 1 of its geologic history (see below). Ash- and soil-mantled dip surfaces of lava flows extend from the caldera rim down to approximately 100 m above sea level. Below this elevation wave erosion and colluvial processes have truncated the flows and exposed them in section. Few of these flows are laterally extensive, although separate exposures may be parts of the same eruptive event (Fig. 4A). A few dikes were observed, and undoubtedly more would be found by systematic mapping. One forms a very narrow point on the coast ~1.3 km south of Anatahan village (Fig. 2A), and another occurs along the south coast (Fig. 4C).

On the south flanks, banked unconformably against these truncated flows are indurated breccias. These breccias are extensive, in some locations comprising most of the lower slopes (Fig. 4B). They are currently being eroded along with the flows and pyroclastic layers. The unconformity separates lava flows dipping south ~20° from overlying, poorly bedded, indurated breccia and other units (Fig. 4C). Close examination showed that the truncated edges of the pre-breccia units were rounded and worn smooth prior to, or perhaps during, deposition of the breccia.

Fig. 2. (A) Shaded relief image illustrating the overall morphology of Anatahan. Digital Elevation Model (DEM) digitized from 1960 1:25,000 U.S. Army Map Service (Far East) topographic map of Anatahan (Sheet 3371 III SE, Series W843), and georectified to WGS-84 datum. Contour interval = 100 m. *Dashed line* indicates 100 m bathymetric contour. (B) Mosaic of air photos collected in 1952 (not ortho-rectified). *Numbers*, *arrows*, and *boxes* indicate views of, and areas covered by, subsequent figures. (C) Perspective view of shaded relief image draped over DEM, viewed from southeast (no vertical exaggeration).

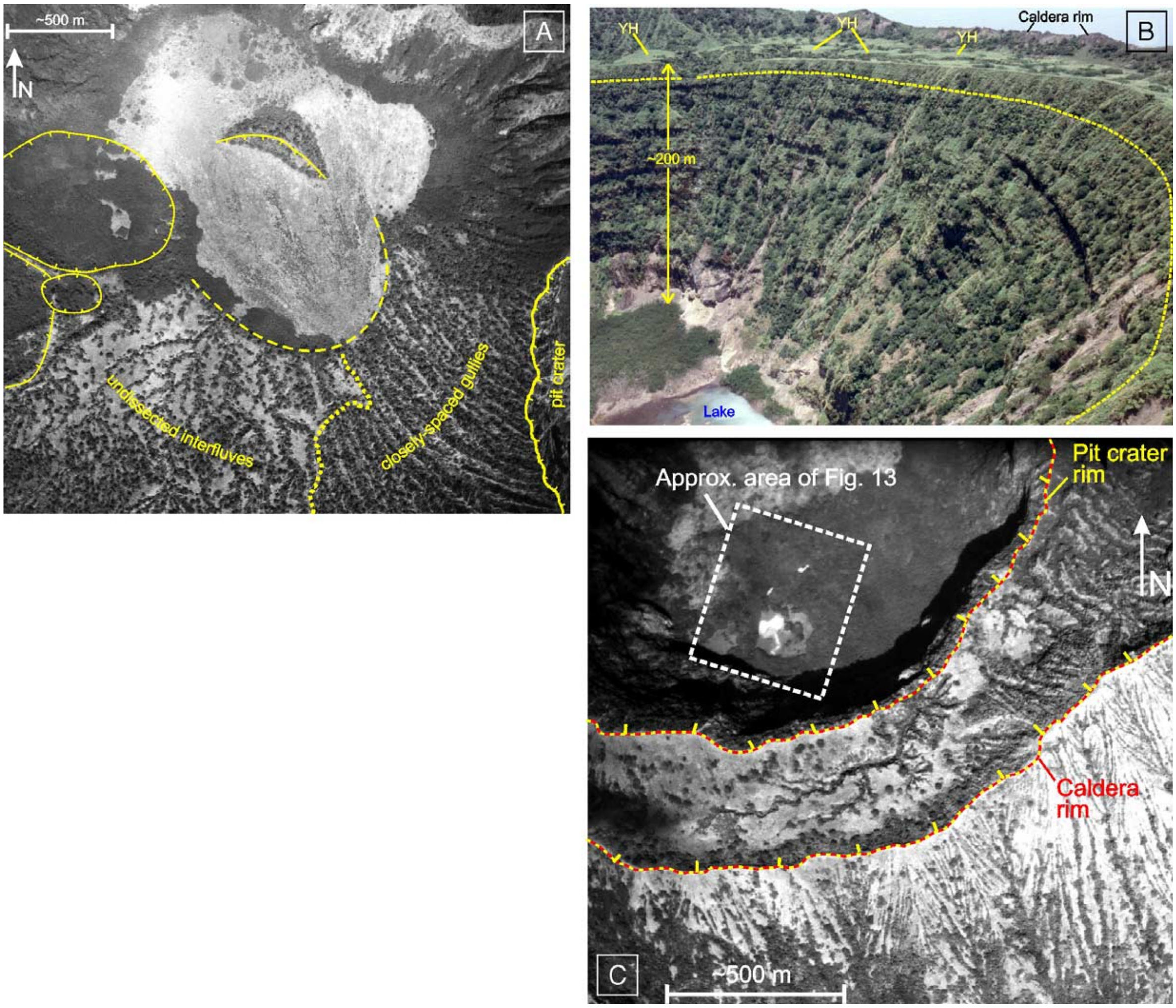

Fig. 3. A) Portion of stereo air photo showing ramp of material extending from caldera floor to south caldera rim (out of image at bottom). Note difference in nature and degree of gully dissection (divided by *dotted line*) in southwest and southeast portions of the ramp. *Dashed line* indicates truncated downslope edge of ramp. *Lines with tick marks* indicate crater rims of stage 2 intra-caldera vents at left (see text and Fig. 8A), and the pit crater at right. B). Oblique view to southeast across the south part of the pit crater (June 1990). Note the layers exposed in the pit crater and their relatively horizontal orientation, indicating emplacement in an enclosed depression (presumably the caldera). *YH* and *dashed line* indicate undissected remnants and base, respectively, of the young hydromagmatic deposit. C) Portion of stereo air photo showing the south part of the pit crater in January 1952. Note the nearly white region devoid of vegetation, suggesting activity similar to that observed between 1990 and 2001.

Unsystematic sampling of flows and pyroclastic deposits exposed in gullies and along the coastal shelf yielded rocks with chemical compositions ranging from nearly basalt to dacite (Fig. 5A). With one exception, all the samples, regardless of volcanic stage (see below), fall on a relatively straight trend on a plot of wt.% (Na_2O+K_2O) vs. SiO_2. A comprehensive discussion of Anatahan geochemistry is presented by Wade et al. (2005-this issue).

A few large lava flows extend the southwest coastline outward a few hundred meters (Figs. 2 and 6). They apparently fill erosional gullies in addition to extending beyond the rest of the coast, so we interpret them to be younger than most of the flows exposed in

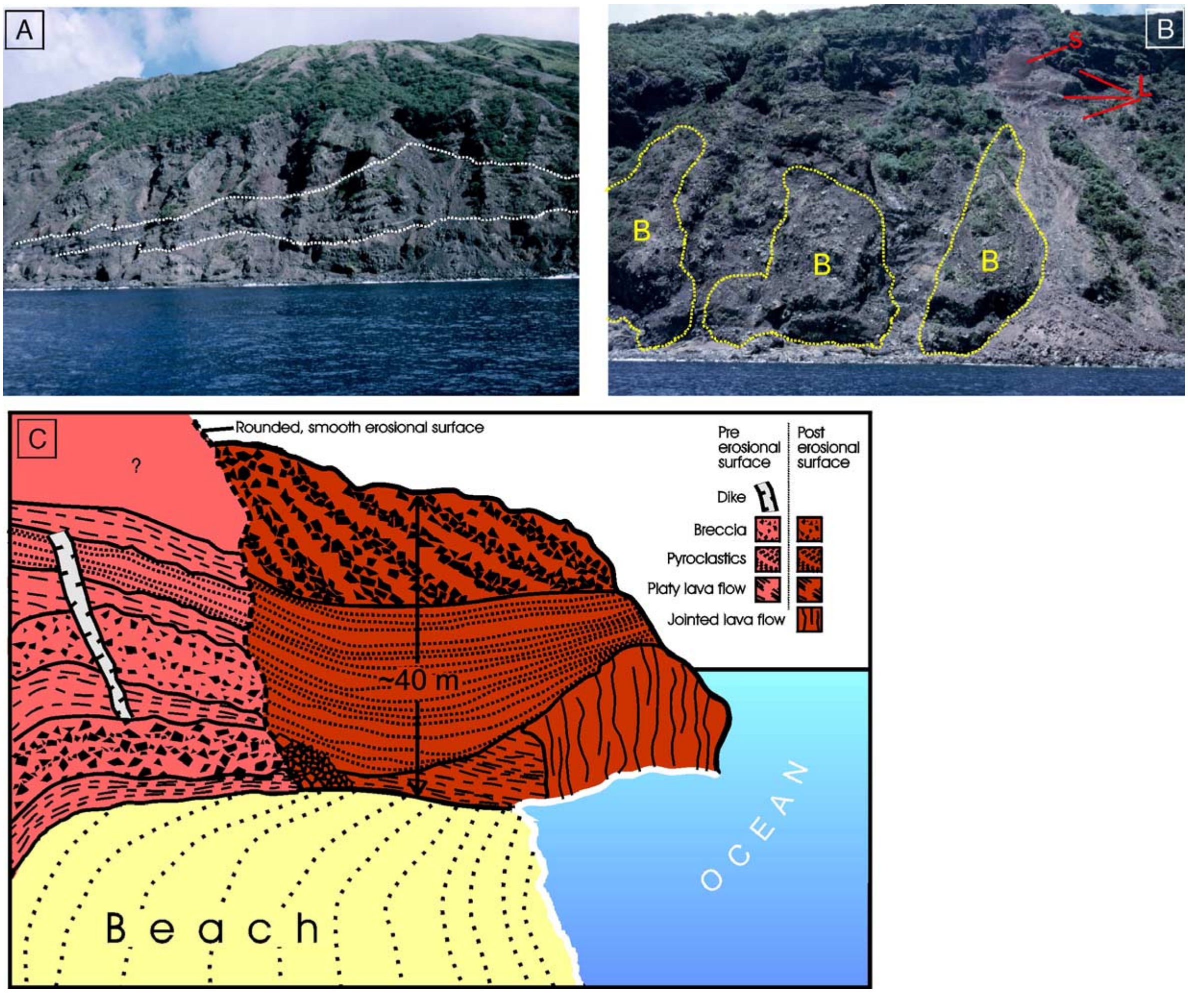

Fig. 4. The south flank and coast. A) View from offshore near the southeast coast. Note that no dip slopes extend to sea level; instead, the lower flanks expose truncated layers. At least one set of flows can be traced for a few hundred meters and is bracketed by the *dotted lines*. B) Closer view of the south flank. Note complex interbedding of lava flows (*L*) and scoria deposits (*S*). Note also the indurated breccia (*B*) that comprises a considerable percentage of the slope: the breccia is currently being eroded into discontinuous outcrops. C) Sketch (view to east) of small promontory exposing the contact between truncated units and indurated breccia (see Figs. 2 and 9 for location).

the flanks. They have therefore been grouped into stage 2 of our geologic sequence (see below).

The largest of these flows, at the southwest corner of the island, was examined from offshore (Fig. 6B). It thickens toward land and has crude columnar joints. What appears to be a flow margin can be traced upslope in an erosional valley; however, this was not field checked. Complicating the interpretation is a thick scoria layer that also occurs on this peninsula. The scoria appears to thicken as the flow thickens, suggesting an association between the two that could argue for a local rather than upslope source for the lava flow.

Much of the northern coastline did not afford access from the ocean, so most of our observations of the north flank were from a few hundred meters offshore or from a helicopter. In general the stratigraphy appeared to be similar to that of the south coast, with what appear to be interbedded lava flows, pyroclastic deposits, and volcaniclastic deposits exposed in a steeply eroded flank. Near the northeast corner of the island, as well as below the

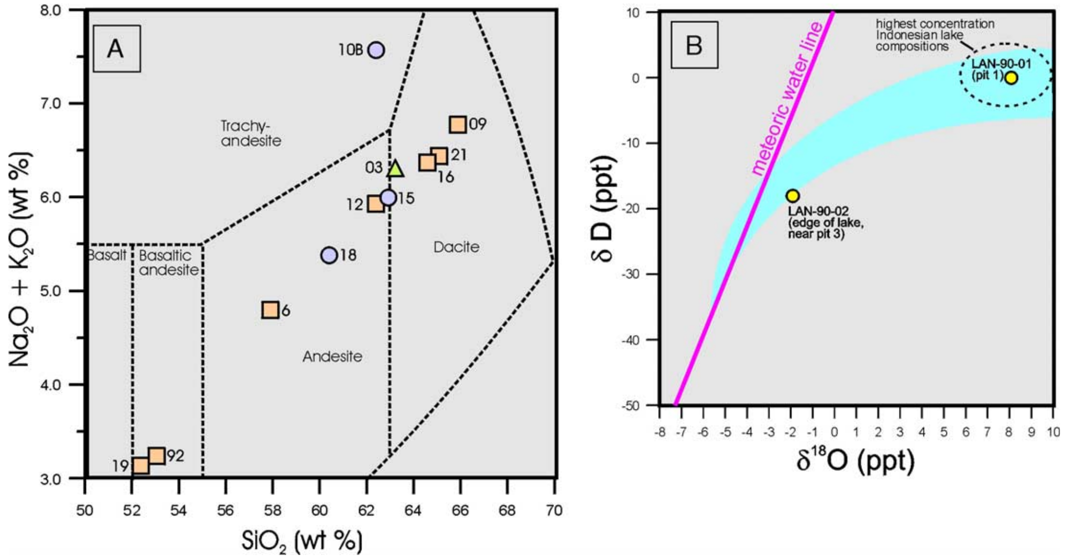

Fig. 5. Geochemistry of collected samples. A) Plot of wt.% Na_2O+K_2O vs. SiO_2 (after Cox et al., 1979) for 11 Anatahan rock samples. *Squares*, *circles*, and *triangle* represent samples from stages 1, 2, and 3, respectively. Numbers next to symbols refer to the last two digits of the full sample numbers (Wade et al., 2005-this issue), and correspond to sample locations in Fig. 12. XRF analyses by Dave Siems. B) δD vs. $\delta^{18}O$ for two water samples collected April 19, 1990 from pit 1 (LAN-90-01) and from the lake near pit 3 (LAN-90-02; see Fig. 13 for locations). Data are plotted with Indonesian volcanic crater lake trends from Varekamp and Kreulen (2000). *Solid line* is the range of meteoric water compositions, *dashed oval* is the range in values for warm, highly concentrated volcanic lakes in Indonesia, and *gray shading* indicates the mixing trend between them.

lowest point on the north caldera rim, we observed sequences of relatively thin, uniform-thickness, dark-colored lava flows separated by apparent clinker layers (Fig. 7). These appear to be ‘a‘ā flows and suggest a basaltic composition.

6. Eruptive vents

The many scoria and ash layers exposed in the steep outer flanks (which make up stage 1 of our geologic sequence) indicate the presence of numerous

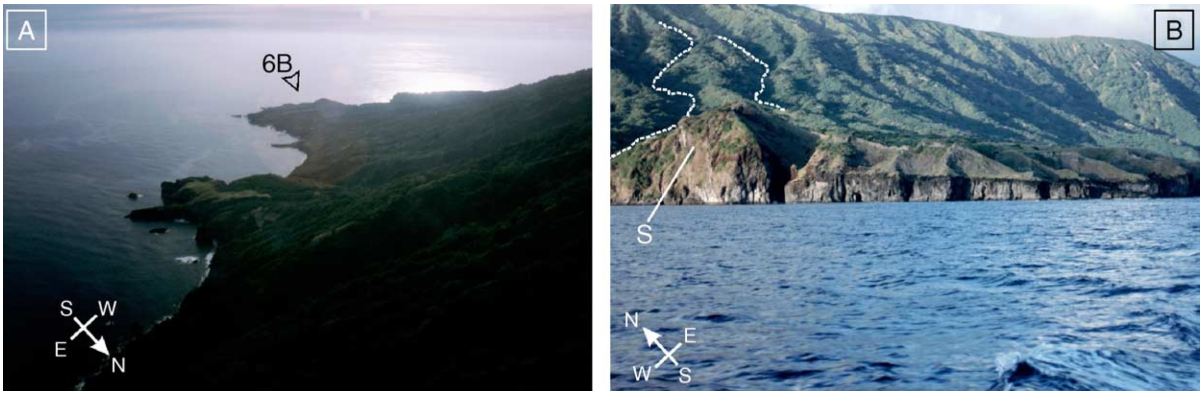

Fig. 6. Young valley-filling flows on the southwest flank. A) View to southwest from above the south caldera rim, showing peninsulas extending beyond the otherwise relatively straight south coastline. Each peninsula consists of a single thick flow. *Arrow* indicates approximate location and direction of view shown in Fig. 6B. B) View to northeast toward thick flow forming peninsula at southwest corner of island. Note the crude columnar jointing and the overlying scoria (*S*). *Dashed lines* indicate approximate upslope flow margins.

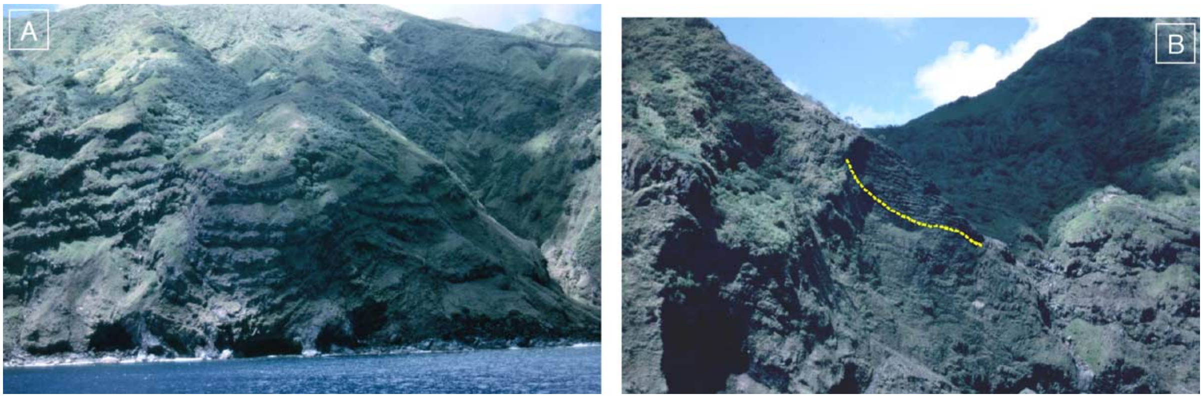

Fig. 7. Photos of relatively young, thin, dark-colored, regularly bedded flows on the north coast. Note that both sequences consist of alternating slope- and cliff-forming layers, which we interpret to be interbedded ‘a‘ā clinker and core, respectively. A) View from offshore of the northeast corner of the island. B) View from offshore of the lowest point on the north caldera rim. *Dotted line* indicates base of sequence of ~17 thin-bedded flows.

eruptive vents within the main body of the volcano. In addition, we identified 22 pyroclastic deposits where vent structures can be identified; these are included in stage 2 of the geologic sequence because of their morphological preservation (Figs. 8 and 9). Five occur within the caldera, six are on the eastern flank, and two are on the western flank. The remaining nine are along the southern caldera margin, but we are less confident of their interpretation.

Young vents were identified on the basis of positive topography of scoria cones and ash rings, closed topographic depressions of craters, and lower amounts of erosion relative to nearby surfaces. We did not visit most of them. All the young intra-caldera vents are located in the western part of the caldera and are identified by roughly circular topographic forms and partially buried scoria and ash rims (Figs. 3A and 8A). One forms a small arcuate hill standing ~35 m above the surrounding surface. This hill is slightly concave to the southwest, indicating a now-buried vent in that direction. When extended, the arc of this rim corresponds to the arcuate downslope edge of the ramp of material that extends to the south caldera rim (see above). A portion of another tuff ring, approximately 20 m high, isolates the southwestmost part of the caldera (Fig. 3A). The smallest intracaldera vent (Fig. 8B) is on the rim of a larger vent and in 1990 hosted the only fumarolic activity (sulfur deposition and active steaming) outside of the pit crater.

One clearly identifiable young vent on the west flank forms a northwest–southeast-elongated crater approximately 1.5 km east of Anatahan village (Fig. 8C). Dense vegetation obscured our view of any volcanic structure while in this depression, but we were able to confirm a nearly horizontal floor. Approximately 1 km southeast of Anatahan village is a ~500-m-wide region of relatively undissected planar topography that dips roughly northeast. We have interpreted this as the remnant of a relatively young vent.

The extracaldera vents located on the eastern flanks are identified by closed or nearly closed depressions in the otherwise steeply dipping outer volcano slopes (Fig. 8D). The largest of these is low enough on the flanks to have been truncated by marine erosion; we refer to it as the southeast crater (Fig. 8E, F). The erosion has exposed a ponded lava flow and probable feeder dike beneath the crater floor. The flat surface of the crater floor afforded the only feasible location on this end of the island to set up a radial tilt array (see below), although access from the ocean was treacherous. The west flank, intra-caldera, and east flank vents, along with the pit crater, form a broad west–northwest to east–southeast band that is roughly parallel to the long dimension of the island. The elongate shape of the island may be at least partially due to this distribution of subaerial vents (W. Chadwick, pers. commun., 2004).

The south caldera rim vents are identified from arcuate ridges in contours and local saddles along, and just below, the caldera rim as seen in stereo air photos (Fig. 9). We are less confident of these being eruptive

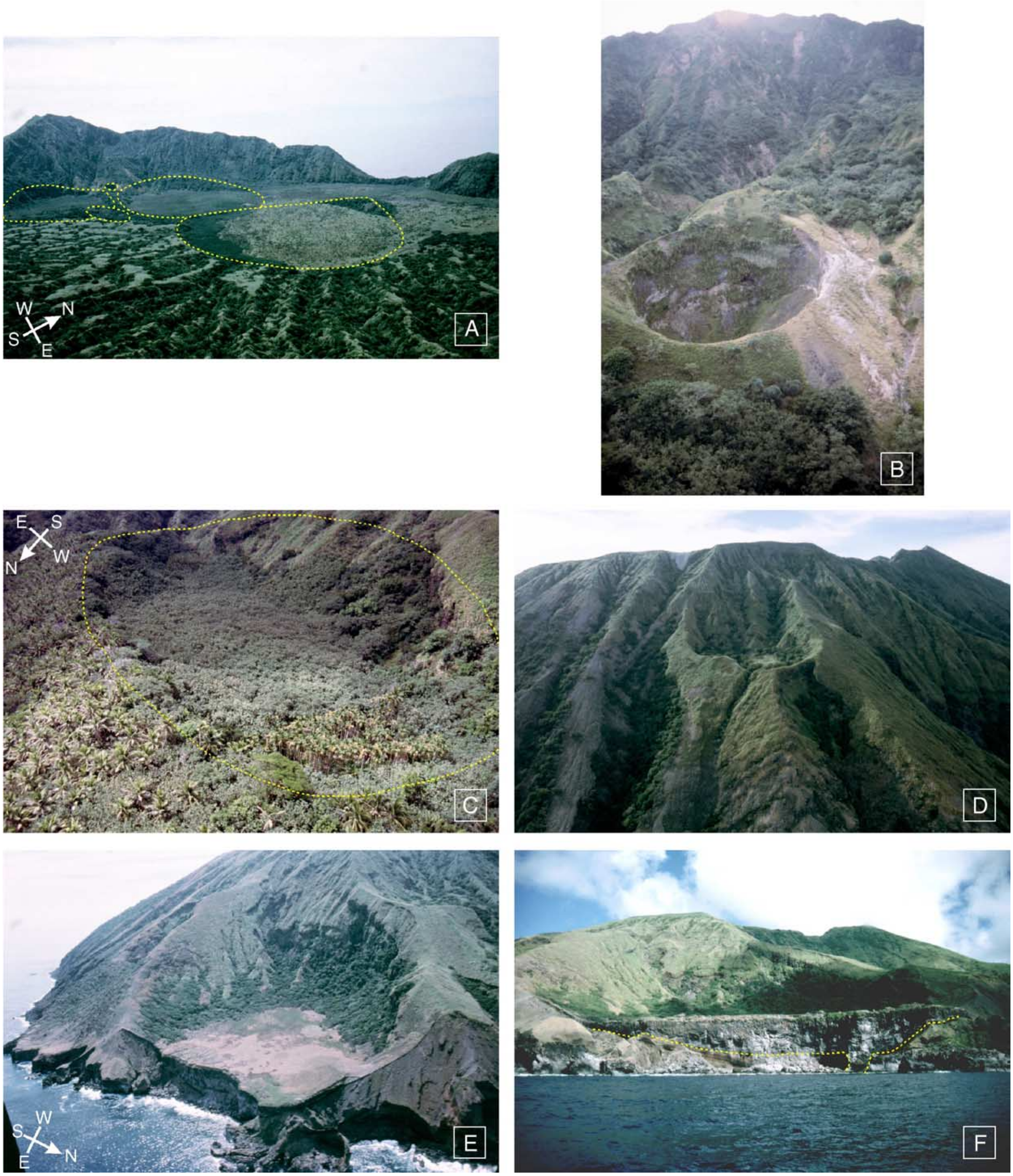
W
N
S
E
A
B
E
S
N
W
C
D
S
W
E
N
E
F

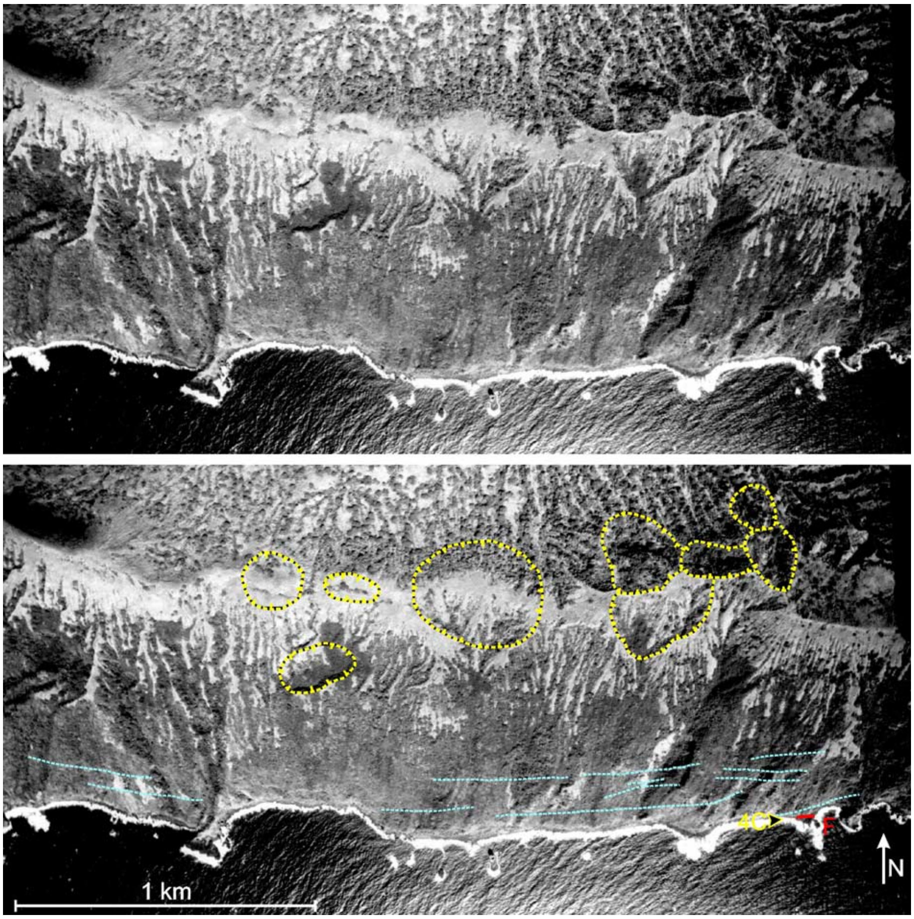

Fig. 9. Portion of January 1952 stereo air photo of the south flank and coast with and without annotation showing lineaments (~*straight dashed lines*) and possible crater rims of geologic stage 2 (*curved dashed lines* with *tick marks* pointing into craters). *4C* and *arrow* indicate location and view of Fig. 4C and breccia-mantled possible fault (F), traced with *solid line*.

craters than we are of the others described in this section.

7. Flank lineaments

The steep, south-dipping unconformity along the south coastline (Fig. 4C) may be a fault scarp. Numerous other lineaments are visible in air photos along the south flanks (Fig. 9), all aligned east–west, roughly parallel to the unconformity observed on the coastline. Some of the lineaments are dark and others are light. They may indicate vegetation variations due to different amounts of water retention along fractures. Other than the unconformity described above, we visited none of the flank lineaments, and no offset

---

Fig. 8. Photos of vents associated with eruptive stage 2. A) Ash and scoria rings in the west part of the caldera. The rims (*dotted lines*) are almost buried by sediment washed into this part of the caldera. The smallest of these vents (against the far western caldera wall) is shown in close-up in B. B) Small intra caldera vent erupted through rim of larger pre-existing vent. The light-toned material on the right hand (north) part of the rim is sulfurous; minor steaming was observed here in 1990. C) Elongate crater ~1.5 km east of Anatahan village. *Dotted line* indicates rim, and coconut trees in foreground are ~20 m tall. D) Small crater approx. halfway up the southeast flank. Downslope rim is breached by a small stream gully. E) View of large vent on southeast coastline (southeast crater). F) View to northwest of southeast crater from offshore. Note crater-filling lava flow. The base of the flow and its feeder dike are highlighted by the *dotted line*.

across them is visible in the air photos. One non-tectonic interpretation is that these represent relatively straight truncations of cliff-forming lava flow units. Similar linear features occur along the north flank as well, but their orientation is more oblique to the coastline.

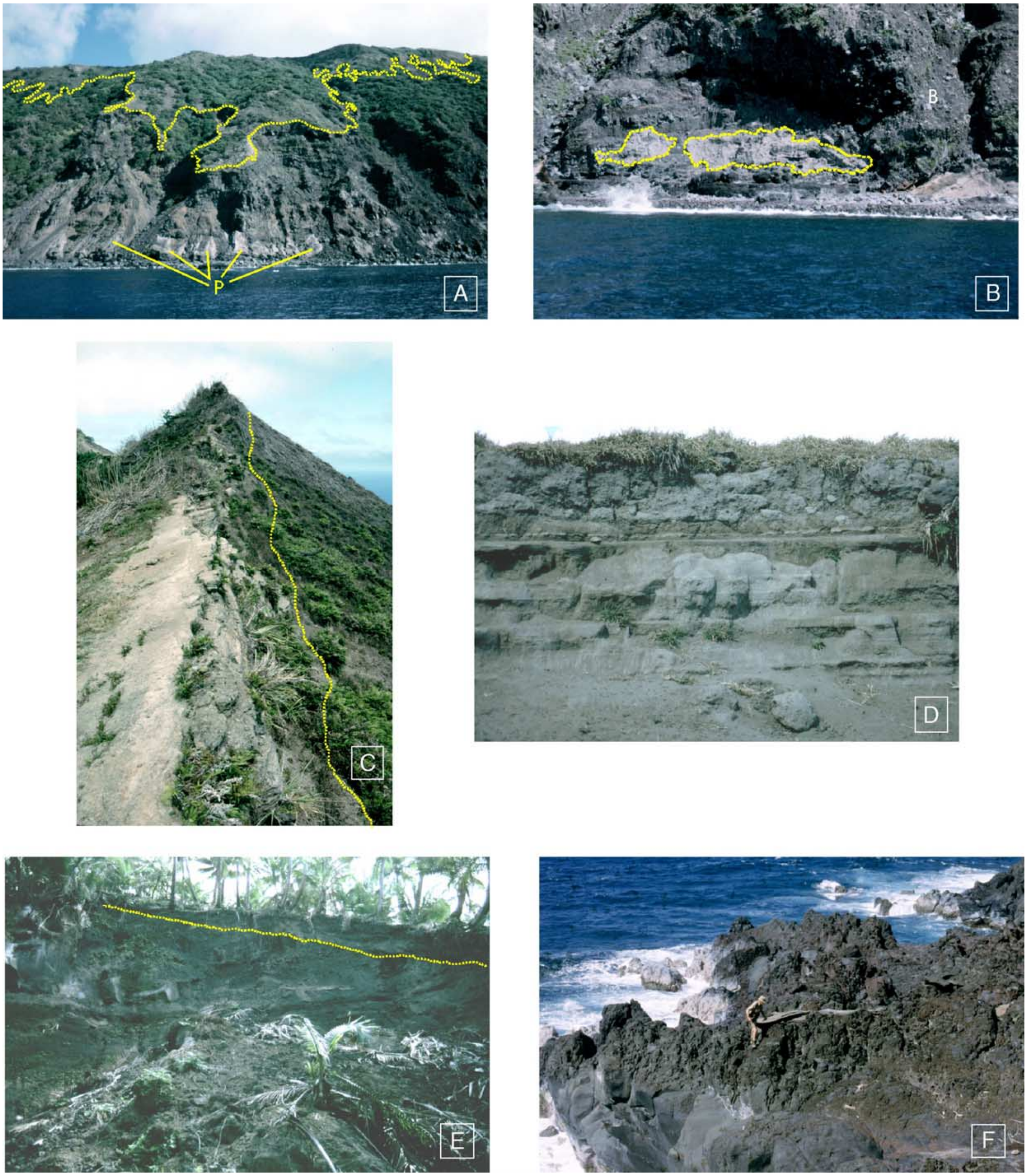

8. The youngest pre-2003 hydromagmatic ash

Prior to 2003, much of the island was covered by 1–10 m of light colored ash. The ash unit is light tan to gray in color, bedded, and blankets underlying surfaces at most outcrops. Because some of the ash beds contain abundant accretionary lapilli, we consider the unit as a whole to be hydromagmatic. It is poorly indurated and can be scraped away easily with a hammer or shovel. The unit blankets the upper flanks outside the caldera (Fig. 10A), all lower surfaces within the caldera, and most of the west flanks of the island. The only locations where it does not occur are the steep inner caldera and pit crater walls, most of the steep north flank, and the lower outer flanks where mass wasting and wave erosion are prevalent. Evidence indicates that it once covered some of these locations as well (Fig. 10B).

The hydromagmatic ash unit forms the top of the section at the pit crater rim, where it is an estimated 10–15 m thick (Fig. 3B), and it dips radially away from the rim. The ash mantles, to a depth of a few meters, the gradual slopes extending from the caldera floor to the south caldera rim (Figs. 3A and 10C). Gullying of the ash in the caldera wall produces distinct patterns in air photos (Fig. 3A), because light-toned grass grows on the interfluves while dark-toned trees and bushes grow in the gullies. The unit is much less conspicuous along the north caldera margin, where there is a distinct break in slope between the floor and wall. Outcrops on the north rim tend to dip away from the caldera.

Outside the caldera, the hydromagmatic unit varies considerably in thickness and complexity. In the floor of the southeast crater, it is >1.5 m thick and presents numerous internal variations in structure and grain size (Fig. 10D). Near Anatahan village, on the northwest corner of the island, it is <1 m thick, and internal variations are much less distinct (Fig. 10E).

The hydromagmatic unit occurs in small outcrops along the coastal shelf, where wave energy is considerable (Fig. 10A, B, F). We noted one location where the unit was banked against a ~2 m-diameter boulder sitting on the shelf. We have no absolute age data, but survival of this barely indurated unit in such a high energy environment suggests a young age, perhaps only a few hundred years. Driver (1992) notes that in a history published in 1887, Mariana people say of Anatahan "...that in times past, there was a volcano, of which only the crater remains." Whether this refers to eruptions in times past is unclear. The May 2003 eruption gives the young hydromagmatic unit more significance, because the 2003 ash blanketed the island in a similar fashion (Fig. 11; Nakada et al., 2005-this issue; Pallister et al., 2005-this issue).

9. Sector collapse?

Most of the subaerial Northern Mariana volcanoes in general are radially symmetric (Kuno, 1962), in contrast to Anatahan, which is distinctly elongate. This elongate shape may be due to the coalescence of two closely spaced volcanoes (Tanakadate, 1940). A second process that has been shown to alter an originally radially symmetric volcano is sector collapse (e.g. Fairbridge, 1950; Siebert, 1984; Siebert et al., 1987). Evidence that Anatahan may have suffered sector collapse(s) is limited. First, both the north and south flanks and coastlines are quite straight (Fig. 2), not convex-outward as on most stratovolcanoes, but also unlike the concave-outward morphology typically produced by sector collapses.

Near-shore bathymetric data are limited to a few soundings associated with the 1960 U.S. Army Map Service 1:25,000 topographic map, and bathymetric

Fig. 10. The young, pre-2003, hydromagmatic ash. A) The south flank viewed from a few hundred meters offshore. The young ash mantles the uppermost slopes and planezes between valleys (outlined by *dashed line*). Note also the light-toned patches (P) banked against the lower slopes just above the coastal shelf. B) Closer view of additional patches of young ash (*outlined*) along the south coastal shelf. Here the ash lies unconformably against truncated lava flows and pyroclastic deposits of stage 1. *B* indicates indurated breccias which also unconformably overlie older stage 1 rocks. C) View eastward along the south rim of the caldera. The lightest deposits are the young ash, dipping west into the caldera. The thickness here is 1–2 m (*dotted line* approximates base of unit). D) Upper 2 m of section through ash in the floor of the SE crater. Note the horizontal bedding. E) Ash exposed near the coastline on the west end of the island. Young ash comprises only the uppermost ~1 m (above *dotted line*), here unconformably overlying locally derived scoria layers. F) Remnant of young ash (just right of geologist) emplaced on wave-washed lava flow outcrop a few hundred meters north of Anatahan village. This location is clearly within the reach of waves, and close inspection of the contact with the underlying flow showed no intervening units; the marine-erosional situation at the time of deposition was apparently the same as in 1990, when this photo was taken.

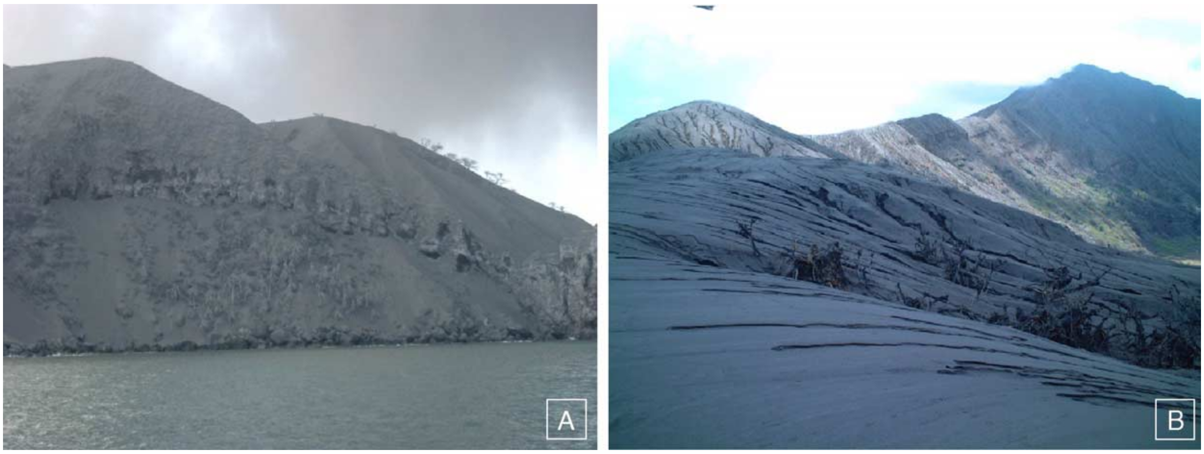

Fig. 11. Photos of 2003 Anatahan ash deposits for comparison with young, pre-2003 hydromagmatic ash. A) 2003 ash mantling all but the steepest slopes near the west end of the island (photo taken May 21, 2003 by D. Hilton). B) Ash-coated slopes along the south caldera rim (photo taken July 19, 2003 by S. Nakada).

contours are necessarily generalized. In fact only a 100-m contour is available, and its shape shows no indication that sector collapse occurred. Furthermore, off most of the north and south coasts the 100-m bathymetric contour is 3–4 times as far from the coastline as the 100-m topographic contour is. This means that near-shore submarine slopes are considerably less steep than subaerial slopes. Deeper bathymetry does not indicate the presence of sector collapse scars (Embly et al., 2004; Chadwick et al., 2005-this issue).

One unit that may be related to sector collapse is the breccia that we observed on many of the lower southern flanks (described above; Fig. 4B, C). The unit is indurated and currently being eroded, suggesting that the conditions that led to its formation no longer exist. Perhaps this breccia formed during sector collapse, although this is only speculation. Another explanation is that the shelf-like near-shore bathymetry was cut during a lower stand of relative sea level (e.g. Stearns, 1978; Lambeck, 2004), coincident with the breccia developing against what would have been higher sea cliffs.

10. Interpretation and eruptive history

Fig. 12 is a geologic map based on our preliminary examination of the island. We divided the rock units into three stages. Most of the outer flanks and caldera walls consist of stage 1 lava flows, pyroclastic rocks, and volcaniclastic sediments that have been exposed by wave and water erosion, landsliding, and caldera formation. These units all dip away from the volcanic center. Except for a few dikes, all exposed stage 1 rocks are extrusive. As noted above, we were unable to resolve the question of how many volcanic edifices once existed. Meijer et al. (1983) report radiometric ages for two lava flows exposed on the coastline of Anatahan. An andesite near the northeast corner of the island has an age of 1.31 ± 0.21 Ma, and a basaltic andesite just south of Anatahan village, near the northwest corner of the island, has an age of 0.40 ± 0.11 Ma. Both correspond to locations that we have mapped as stage 1.

The stage 1 rocks were truncated by both gradual and catastrophic erosion. Water, wave, and gravitational processes helped to produce the steep, gullied surface of the volcano, although even undissected surfaces probably had relatively steep initial dips. These processes continue today; we observed numerous small landslides off the slopes, some undoubtedly triggered by herds of goats. An almost certainly catastrophic event was formation of the caldera. Plan-view caldera morphology suggests two collapses spatially close enough to coalesce. Most of the inner walls of the caldera are eroded to about the same degree as the outer flanks. We interpret this to mean that caldera formation was not recent. Extending the outer flanks upward beyond the current caldera

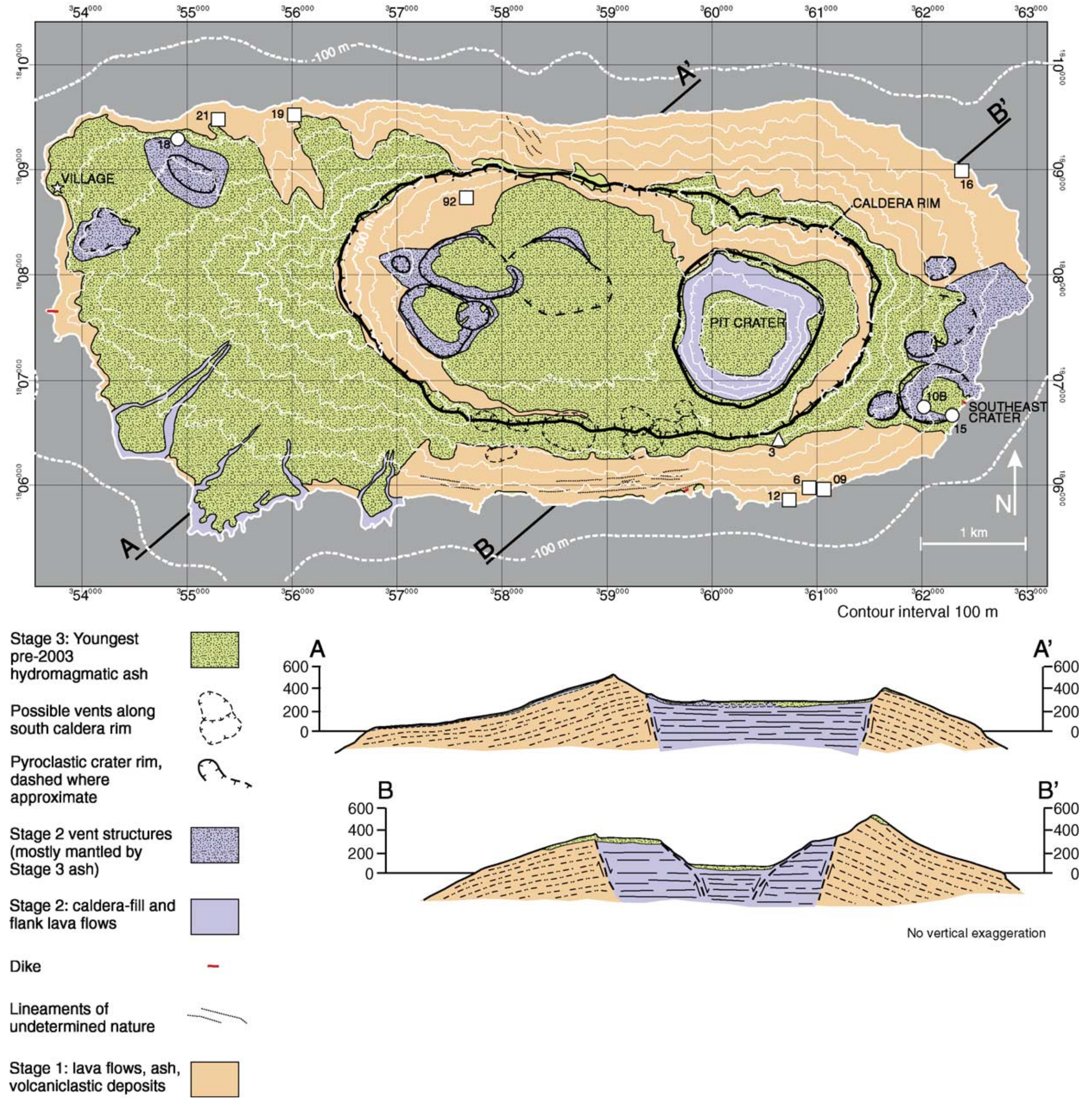
A
A'
B
B'
CALDERA RIM
PIT CRATER
VILLAGE
SOUTHEAST CRATER
-100 m
500 m
21
19
18
92
16
10B
15
3
6
09
12
N
1 km
Contour interval 100 m
600
400
200
0
No vertical exaggeration
Stage 3: Youngest pre-2003 hydromagmatic ash
Possible vents along south caldera rim
Pyroclastic crater rim, dashed where approximate
Stage 2 vent structures (mostly mantled by Stage 3 ash)
Stage 2: caldera-fill and flank lava flows
Dike
Lineaments of undetermined nature
Stage 1: lava flows, ash, volcaniclastic deposits

Fig. 12. Reconnaissance geologic map of Anatahan. Cross sections are highly conjectural. *Squares*, *circles*, and *triangle* show locations of samples plotted in Fig. 5A for stages 1, 2, and 3, respectively. Numbers next to symbols refer to the last digits of the full sample numbers (Wade et al., 2005-this issue).

margin produces a volcano ~1200 m high, almost twice the current highest elevation.

A second, but only speculative, catastrophic event was sector collapse. As noted above, only limited evidence suggests this may have occurred, but if so, it could have contributed to the development of straight north and south coasts as well as to deposition of the breccia unit.

All eruptive events and their associated products that postdate the caldera but predate the young, pre-

2003 hydromagmatic ash have been grouped into stage 2. The western two thirds of the caldera has a near-horizontal surface, and the pit crater exposes relatively horizontal lava and ash layers (Fig. 3B). These relations indicate that part of stage 2 included caldera infilling. These units are exposed at the base of the pit crater, so the original caldera depth was at least 200 m greater than it is today. The formation of the pit crater itself was an event that occurred during stage 2, as were the eruptions from vents in the western part of the caldera. Toward the end of the caldera-filling activity, pyroclastic units mantled and banked against the south caldera wall. These form the ramp-like surface currently being gullied (Fig. 3A). The marked difference in gully density between the southwest and southeast parts of this ramp may reflect two distinct events.

Extra-caldera activity during stage 2 included emplacement of the valley-filling flows on the southwest flanks to form the relatively uneroded peninsulas at the southwest corner of the island. These flows post-date the degradation of the outer flanks, but their relative timing with respect to caldera formation and

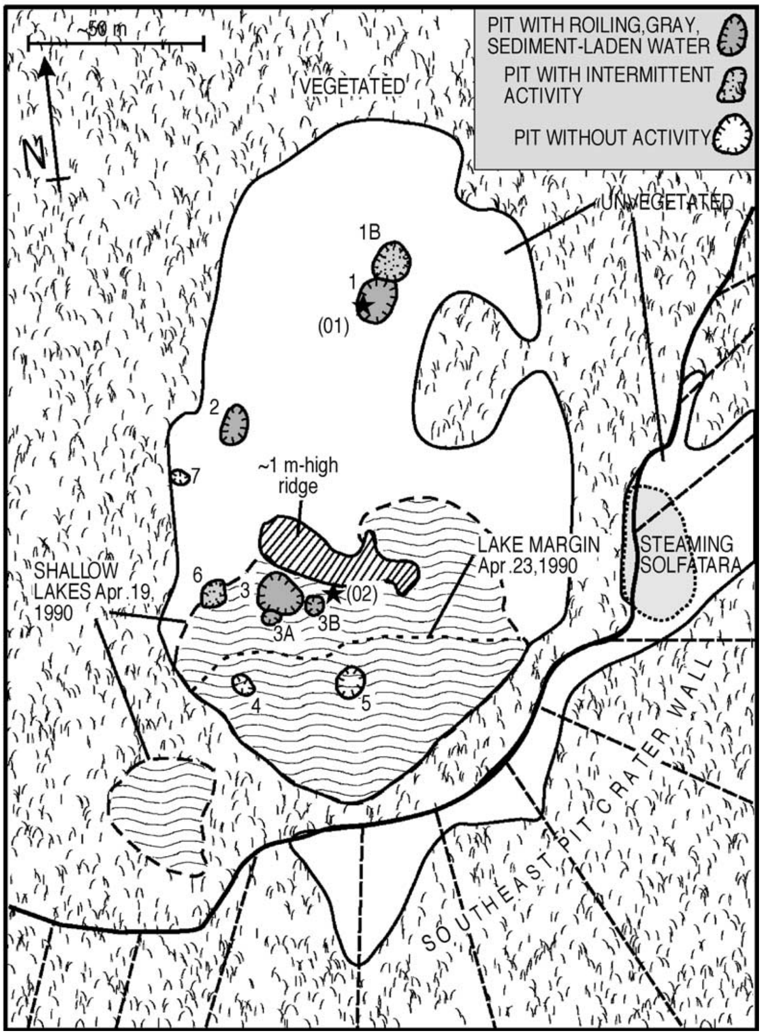
~50 m
N
VEGETATED
PIT WITH ROILING,GRAY, SEDIMENT-LADEN WATER
PIT WITH INTERMITTENT ACTIVITY
PIT WITHOUT ACTIVITY
UNVEGETATED
1B
1
(01)
2
7
~1 m-high ridge
LAKE MARGIN Apr.23,1990
STEAMING SOLFATARA
SHALLOW LAKES Apr.19, 1990
6
3
3A
3B
(02)
4
5
SOUTHEAST PIT CRATER WALL

Fig. 13. Sketch map of geothermal area in south part of pit crater. Numbers indicate pits referenced in text and Table 2. Note that pits 1–5 existed in April, 1990, and pits 6 and 7 were first noted in June, 1990 and June, 2001, respectively. *Black stars* show locations of water samples collected April 19, 1990 (Table 3), with last two digits of sample numbers in *parentheses*.

intra-caldera activity is undetermined. Finally, the east and west flank and south-caldera-rim vents also are part of stage 2, because they also postdate major erosion of the flanks.

Stage 3 consists of the young, pre-2003 hydromagmatic unit. Its occurrence in high-energy environments supports a young age, perhaps few hundred years. As we noted above, a history written in 1887 (Driver, 1992) mentions a "volcano" on Anatahan "in times past", perhaps referring to a witnessed eruption. We have not identified a source vent for this deposit but suggest it was the pit crater, based on six lines of evidence. First, the unit forms a raised rim around most of the pit crater, and in almost all directions the surface dips away from this rim. Second, the greatest thickness (10–15 m) occurs in the upper walls of the pit crater (Fig. 3B). Third, the pit crater was the location of the greatest amount of remnant volcanic heat (the geothermal area). Fourth, other than low on the coastline, this is the only location where the ground surface is close to the water table, affording easy access of erupting magma to external water. Fifth, the 1887 historical account (Driver, 1992) mentions that "...only a crater remains" of the volcano (eruption?) from times past. Sixth, the vent for the 2003-to-current eruption is within this crater. As noted above, the current eruption has produced an ash unit resembling the young hydromagmatic unit. We emphasize that the raised rim of the pit crater is underlain by older, similar-looking ash layers as well, so prior, similar events probably occurred.

11. The seismic crisis of spring 1990 and observations of geothermal activity from 1990 to 2001

Fieldwork on Anatahan began because of a seismic crisis in March and April, 1990 (BGVN, 1990a). Beginning on March 28, 1990, earthquakes were felt by the island's residents and detected by the US Geological Survey's National Earthquake Information Center (NEIC). Seven earthquakes > M 4.5 were recorded on March 30 and 31; all but one were located >65 km northeast or north–northeast of the island (BGVN, 1990a). Anatahan had not previously been reported as a source of seismicity.

Residents of the island reported no ground deformation or landsliding associated with the seismic activity. A helicopter overflight at the time noted a change in the pit crater lake from its typical green color to bluish gray, increased fumarolic activity, a fresh landslide in the pit crater, and the odor of H_2S. All 22 residents were evacuated by a U.S. Navy helicopter on April 5. Also on April 5, a M7.5 earthquake occurred approximately 150 km east of Anatahan, in the Mariana trench. This earthquake was apparently unrelated to any activity on Anatahan. The island remains officially evacuated at the time of this writing (April 2005), although people often return to the island to fish and collect fruit bats and betel nuts.

11.1. Geothermal activity, April 19, 1990

When the southern part of the pit crater was first visited on April 19, 1990, we noted a large lake ~100 m wide and a few meters deep, a smaller western lake, and 6 pits (1, 1B, 2, 3, 3A, and 3B) 5–10 m across (Figs. 13 and 14A, B). The area near the pits was devoid of vegetation, and grasses, shrubs, and pandanus trees within an area of 200 m by 100 m appeared to have been killed recently (Fig. 14A, B, D, and E).

Pits 1 and 2 contained vigorously boiling, gray, sediment-laden water (Fig. 14C, D). The water in pit 1 was nearly 100 °C, and a field pH meter gave a reading of 0.7 (Table 2). Pit 1B contained runny gray mud that was slowly upwelling. The lake was large enough to include the pit 3 cluster, two or three of which were active and causing the lake water in the vicinity to have a gray-blue color (Fig. 14F). Along a low ridge of higher ground north of the lake was fresh-appearing explosion debris (Fig. 14F, G), and large angular blocks were found sparsely around the entire geothermal area.

Water samples were collected on April 19, 1990 from pit 1 (sample LAN-90-01) and from the edge of the larger lake (sample LAN-90-02), about 5 m from, but within the plume of, active pit 3 (Fig. 13). Table 3 presents chemical analyses of these samples, which, except for those of sulfur and sulfur species, were performed after the samples had been filtered of sediment. Both samples contain high concentrations

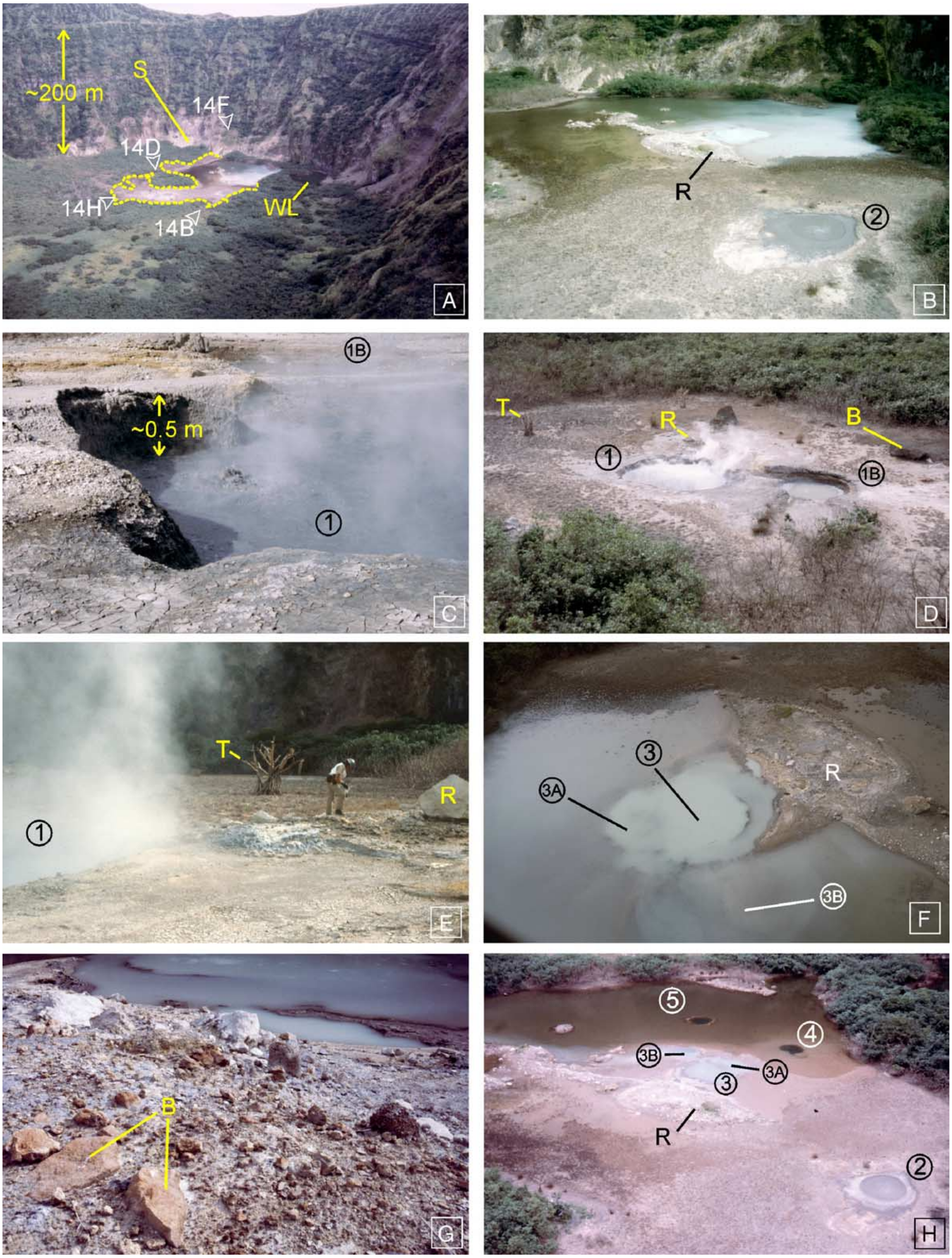
~200 m
S
14F
14D
14H
14B
WL
A
R
②
B
⑴B
~0.5 m
①
C
T
R
B
①
⑴B
D
T
R
①
E
③
③A
R
③B
F
B
G
⑤
④
③B
③A
③
R
②
H

of sulfate, probably due to oxidation of H_2S to SO_2 and then to sulfate (D. Thomas, pers. comm., 2004). The SO_4/Cl ratios are both higher than that of typical seawater (0.16; M. Tuttle, pers. comm., 2004) precluding any significant seawater interaction. $\delta^{18}O$ and δD values were used by Varekamp and Kreulen (2000) to demonstrate mixing between meteoric water and high-temperature volcanic gases. On such a plot (Fig. 5B), LAN-90-02 sits much closer to the meteoric water end of the mixing line, not surprising because pit 3 was at the time submerged within the shallow lake. Interestingly, however, LAN-90-02 also contains considerably higher amounts of almost all elemental constituents despite the dilution by lake water. This may be because pit 3 is located more nearly in the center of geothermal area than is pit 1.

11.2. Geothermal activity, April 23, 1990

By April 23, the lake had shrunk in area so that it did not include the pit 3 cluster. The lake water was clear, revealing two additional but inactive pits within the lake (pits 4 and 5; Fig. 14H). Activity in the active pits 1–3 appeared unchanged except for a slight decrease in the water level in pit 2.

11.3. Geothermal activity, June 1990

In June of 1990 the two shallow lakes had dried up or drained away, and these areas (viewed only from the air) were replaced by what looked to be brown mud. Activity in the pits had not changed significantly since the visit in April 1990 (Fig. 15A, B; Table 2). A sagged area ringed with concentric fractures indicated the position of the future pit 6.

11.4. Geothermal activity, October 1990

In early October 1990 the shallow lake had reappeared (Moore et al., 1991) with "…water that was discolored but not boiling." No visit was made to the crater floor, nor is there mention of the other pits. The situation resembled that of April 19, 1990, with the lake being discolored by its inclusion of one or more active pits, probably the pit 3 cluster.

11.5. Geothermal activity, May 1992

In May 1992 the situation was essentially the same as in June 1990. Specifically, there was no shallow lake, pits 1, 2, and 3 contained vigorously churning, sediment-laden water, and pits 4 and 5 were inactive (Fig. 15C; Table 2; Moore et al., 1993). Pit 6 had developed and was full of sediment-laden water. The highest temperature measured in an active pit was 98 °C. The water level in pit 2, which had been at or just below the general level of the pit crater floor in 1990, was now ~1 m below the pit rim. Vegetation had not encroached to any great degree into the area except for the location of the smaller (western) lake, which was almost completely overgrown.

11.6. Geothermal activity, May 1994

In May 1994 the activity of the pits had not changed significantly. Again, pits 1, 2, and 3 (but not 3A and 3B)

Fig. 14. Photos of geothermal area in pit crater, April 1990. *Circled numbers* correspond to pit numbers in text and Table 2. A) View to southwest April 19, 1990, *S* indicates area of solfataric activity at base of pit crater wall, *dashed line* outlines area of no, and recently killed, vegetation on the crater floor. Western Lake (WL) is separated from the main lake by a narrow vegetated isthmus. Labeled *arrows* indicate approximate locations and directions from which B, D, F, and H were taken. B) View south to lake and hot springs, April 19, 1990. Note the light color of the west part of the lake due to sediment from active pits within the lake. Ridge of higher ground (R) is littered with angular fragments of lake sediments and shown in G. Pit 2 in the right foreground is ~8 m across. C) Close-up view of vigorously boiling pit 1, April 19, 1990. Pit 1B in background visible through steam. D) Air view of pits 1 and 1B, looking northwestward. Block (B) at right is 2 m high by 7 m long. Note the region of dead grass tufts on the flat ground near the pits. Dead pandanus tree (T) and rock (R) also shown in E. E) Ground view to south near west edge of pit 1. The ground behind the geologist consists of dead grass tufts, and the pandanus tree in the background (T) is also dead. Tree (T) and rock (R) also shown in D. F) Air view of pit 3 cluster within the main lake April 19, 1990. Ridge (R) is ~20 m wide by ~50 m long and littered with light-toned, angular fragments of lake sediment (shown in close-up in G). G) Close-up of angular debris littering small ridge of high ground near lake. Largest blocks (B) are 20–30 cm long. H) Similar view as B but taken April 27, 1990. Note that the lake has receded and no longer includes the pit 3 cluster, and therefore, the lake water clarity has increased significantly, allowing pits 4 and 5 to become evident. Note also that water level in pit 2 (lower right) has dropped slightly. *R* indicates ridge littered with angular debris.

Table 2
Activity in pit crater pits April 1990 to June 2001(see Figs. 13, 14, and 15)

Observation date	Pit 1	Pit 1B	Pit 2	Pits 3, 3a, and 3b	Pits 4 and 5	Pits 6 and 7
April 19, 1990 (Fig. 14A–E, G, H)	Surface ~0.5 m below rim, bubbling, near-boiling, pH: 0.7–1.2.[a]	Roiling, sediment-laden water, surface ~1 m below rim.	Gently upwelling sediment-laden water, surface just below rim.	Submerged within lake, pits 3 and 3A producing distinct sediment plumes, pit 3B less obvious. pH of lake water nearby = 1.9–2.0[a].	Not visible (obscured by opaque lake water).	Pit 6 non-existent. Pit 7 non-existent.
April 23, 1990 (Fig. 14F)	Roiling, bubbling, surface ~0.5 m below rim	Roiling, sediment-laden water, surface ~1 m below rim.	Gently upwelling sediment-laden water, surface < 1 m below rim.	All three pits active with roiling, sediment-laden water.	Inactive (within now-clear lake).	Pit 6 non-existent. Pit 7 non-existent.
June 1990 (Fig. 15A, B)	Steaming, sediment-laden water, surface ~0.5 m below rim	Appears inactive.	Sediment-laden water, surface ~1 m below surface	Pit 3: Roiling, sediment-laden water, surface < 1 m below rim. Pit 3A appears inactive, pit 3B sediment-laden, boiling(?)	Inactive, dry.	Pit 6 incipient, consisting of a sagged region. Pit 7 non-existent.
October 1990	n.a.	n.a.	n.a.	Probably boiling, sediment-laden water, submerged within lake.	n.a.	n.a.
May 1992 (Fig. 15C)	Boiling, black, sediment-laden water, $T = 98$ °C (?).	Sediment-laden water (?).	Sediment-laden water, surface ~1 m below surface.	Pit 3: shallow, green-tinted, clear, boiling water. Pits 3A and B appear inactive.	Inactive, dry.	Pit 6: filled with sediment-laden water. Pit 7 non-existent.
May 1994 (Fig. 15D)	Boiling viscous mud, 1.5 m-high splashes, $T = 98.5$ °C, pH = 1.7.[b]	Muddy water, barely bubbling.	Vigorously boiling, sediment-laden water, surface ~2 m below rim, $T = 95.5$ °C, pH = 4.3[b].	Pit 3: bubbling in multiple locations, surface is 1.5 m below rim, $T = 67.4$ °C, pH = 2.7[b] Pits 3A and B appear inactive.	Inactive, dry.	Pit 6: appears dry. Pit 7: non-existent.
June 2001 (Fig. 15E, F)	Boiling viscous mud, surface is 1–2 m below rim, 1.5 m-high splashes, $T = 98$ °C.	Boiling muddy water, $T = 96.7$ °C.	Vigorously boiling, sediment-laden water, surface > 3 m below rim, $T = 100.3$ °C.	Pit 3: bubbling in multiple locations, surface is 1.5 m below rim, $T = 99.4$ °C. Pit 3A gone, Pit 3B inactive. Geothermal area increased.	Inactive, dry.	Pit 6: 1–2 m deep, with water. Pit 7: appears inactive.

n.a. = observations not available.
[a] pH measurement with portable meter.
[b] pH measurement with pH paper.

were active, pits 4, 5, and 6 were inactive, and there was no shallow lake. Pit 1B contained viscous mud. Some vegetation had re-established, with low grasses surrounding pit 2 and a band of vegetation extending across the entire geothermal area, dividing the barren ground in two (Fig. 15D). Temperatures of near

Table 3
Chemical analyses of water samples collected April 19, 1990 from the geothermal area in the pit crater

Sample I.D.	δ 18 H_2O	δD H_2O	SO_4 (aq; mmol)[u]	S=(aq; mol)[u]	Elem. S (mol basis)[u]	δ3/4 S (elem)[u]	δ3/4S SO_4
LAN-90-01	8.1	0	3.6	0.018	13	−0.2	2.6
LAN-90-02	−1.9	−18	6.5	0.0095	0.32	−10.8	3

	SO_4 (mmol)	SO_4/total anions	Cl (mmol)	Cl/total anions	Anions (mmol)	+meq	−meq
LAN-90-01	4.58	0.66	2.37	0.34	6.95	8.23	11.54
LAN-90-02	6.88	0.19	29.19	0.81	36.07	29.99	42.94

	+/−meq	SO_4 (ppm)	Cl (ppm)	F (ppm)	SO_4/Cl	Ca (mmol)	Ca/total cations
LAN-90-01	0.71	440	84	n.d.	5.24	1.55	0.34
LAN-90-02	0.7	660	1035	7.2	0.64	3.49	0.17

	Fe (mmol)	Fe/total cations	K (mmol)	K/total cations	Mg (mmol)	Mg/total cations	Na (mmol)
LAN-90-01	0.1	0.02	0.26	0.06	0.7	0.15	2
LAN-90-02	0.3	0.01	1.92	0.09	3.58	0.17	11.74

	Na/total cations	Tot. cations (mmol)	Ca (ppm)	K (ppm)	Mg (ppm)	Na (ppm)	Si (ppm)
LAN-90-01	0.44	4.6	62	10	17	46	86
LAN-90-02	0.56	21.04	140	75	87	270	84

	Al (ppm)	Fe (ppm)	P (ppm)	Ag (ppb)	B (ppb)	Ba (ppb)	Be (ppb)
LAN-90-01	7.4	5.4	<0.5	<2	480	18	<1
LAN-90-02	5.6	17	<0.5	<2	5500	77	<1

	Bi (ppb)	Cd (ppb)	Co (ppb)	Cr (ppb)	Cu (ppb)	Ga (ppb)	Li (ppb)
LAN-90-01	<10	4	9	<1	60	<5	14
LAN-90-02	<10	1	4	<1	18	<5	170

	Mn (ppb)	Mo (ppm)	Ni (ppb)	Pb (ppm)	Sn (ppb)	Sr (ppb)	Ti (ppb)
LAN-90-01	1400	<10	<5	<10	<10	180	<1
LAN-90-02	8200	<10	<5	<10	<10	470	<1

	V (ppb)	Zn (ppb)	Zr (ppb)
LAN-90-01	38	260	<1
LAN-90-02	26	190	<1

[u] Unfiltered sample.

LAN-90-01 was collected from pit 1, which at the time was boiling, very sediment-laden, and had a pH measured in the field of 0.7–1.2. LAN-90-02 was collected from the shore of the shallow lake, within the sediment plume of, but ~5 m from the center of, pit 3, and had a pH measured in the field of 1.9–2.0. The temperature was not measured but noted to be considerably cooler than that in pit 1. Analyst: Dr. M. Tuttle.

boiling and pH measurements of 1.7–4.3 were recorded in pits 1, 2, and 3 (Table 2; Sako et al., 1995). The water level in all the pits was lower than it had been in 1990 and 1992, with the distance from the crater floor down to the churning surface 2.2 and 1.5 m in pits 2 and 3, respectively.

11.7. Geothermal activity, June 2001

In June 2001 the situation was similar to that in June 1990, May 1992, and May 1994 (Fig. 15E). Pit 1 contained very sediment-laden water with a surface nearly 2 m below the crater floor. Pit 1B

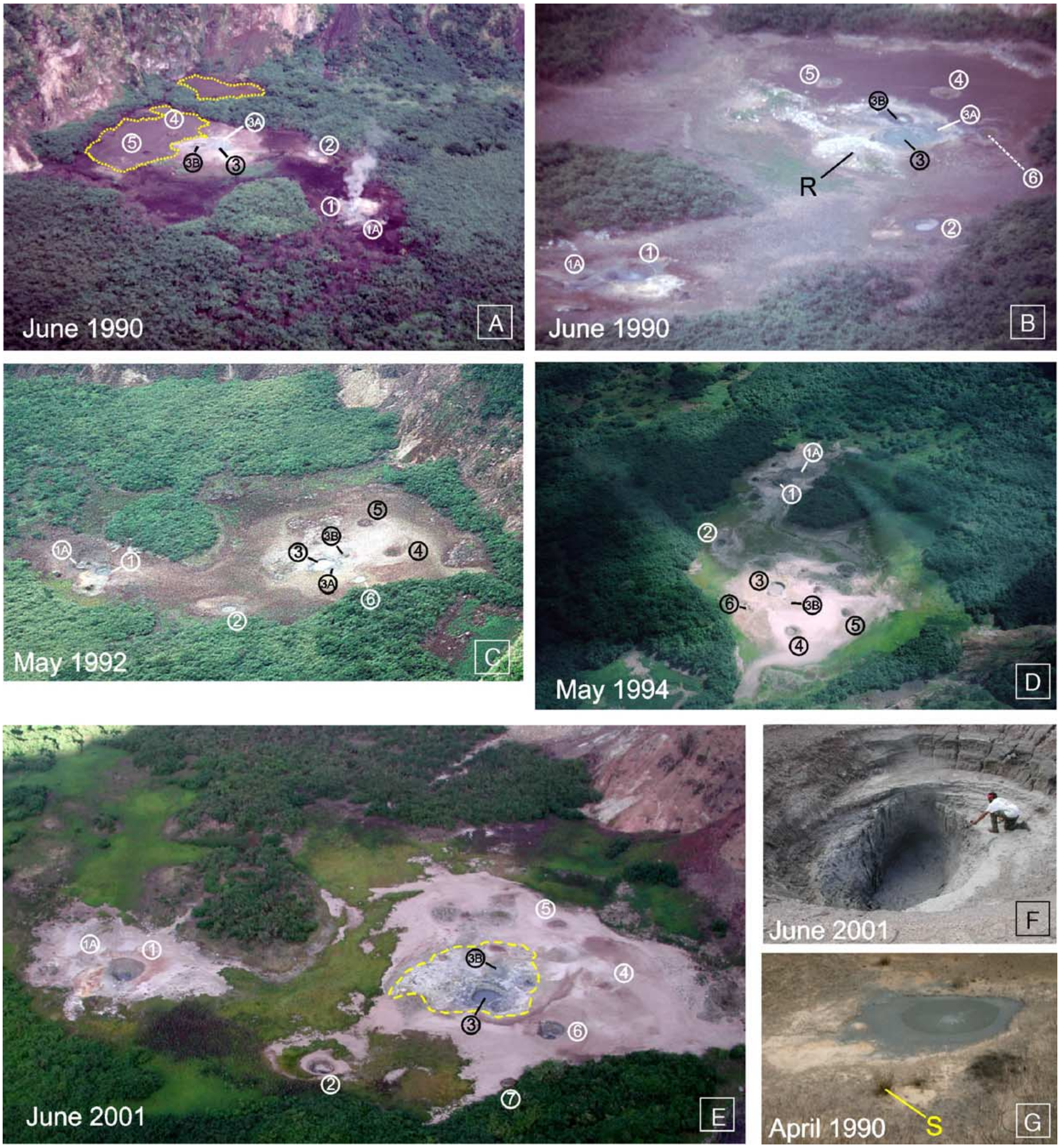

Fig. 15. Photos of geothermal area in pit crater, June 1990 to June 2001. A) View to southwest, June 1990. Vigorous steaming occurs from pit 1 and less vigorous steam comes from pits 2 and 3. The lake has disappeared, replaced by brown mud (April 1990 lake boundaries indicated by *dashed lines*). B) View south, similar to that in Fig. 14B and H. Ridge of angular debris is indicated by *R*, and individual debris blocks show up as light spots nearby. Incipient pit 6 shows up as concentric sag structures. C) View to southeast in May 1992. Pit 6 is filled with sediment-laden water. D) View to northwest in May 1994 (similar to that of Fig. 14F). Pit 3A has been filled in or included into pit 3. E) View to southeast in June 2001. The water level in pit 6 has dropped and pit 7 is evident on the edge of the unvegetated area. Note that the area of bare ground has increased around pits 1 and 1A, whereas around pit 2 revegetation is considerable. The area of increased geothermal activity around the pit 3 complex is outlined by the *dashed line*. F) Close up of pit 2 showing geologist measuring temperature with a thermocouple. Note the depth to the water surface compared to that in April 1990 (G). G) Oblique air photo of pit 2 in April 1990. Note water surface almost to rim of pit. Shrub in foreground (S) is ~1.5 m tall.

contained nearly boiling water (Table 2) with a surface ~1.5 m below the crater floor. The area around pits 1 and 1B was distinctly lighter-toned, apparently due to increased geothermal activity. The surface of pit 2 was >3 m below the crater floor, the walls of the pit had become somewhat funnel-shaped (Fig. 15F), and a temperature of >100° was measured here. Although pit 3 was barely active, its temperature was >99 °C, and the surrounding area had a larger expression of geothermal activity than had been previously observed. Specifically, an area extending 10–30 m away from pit 3 (Fig. 15E) was characterized by numerous small mud pots and inter-connecting channels. Vegetation had become more established in the vicinity of pit 2.

11.8. Summary of geothermal activity, 1990 to 2001

Within the constraints of the infrequent observations and measurements, the activity of the geothermal area within the pit crater was essentially constant from April 1990 to June 2001. Typically the same pits were active from one year to the next, and the major difference was whether or not there was a shallow lake partially filling the lowest area of the pit crater. The appearance of the lake changed markedly depending on whether or not it extended far enough to include pit 3; we could not determine if this was due to variations in rainfall or in geothermal activity. Temperature and pH measurements showed no consistent patterns. Increased geothermal activity around the pit 1 and 3 clusters was noted during the June 2001 visit.

12. Geophysical monitoring from 1990 to 2001

Ground deformation and seismic measurements were made during the visits of April, June, and October 1990, May 1992, May 1994, and June 2001.

12.1. Ground deformation measurements, April 1990

Ground deformation was measured with an electronic distance measurement (EDM) network and two radial tilt arrays. Deformation monitoring stations were limited to locations where helicopter access was available. The EDM network consisted of 6 corner stations and 6 shot lines (Fig. 16A), most of which crossed the caldera. One reflector station was placed near the southwest coast.

A few line-length changes took place some time between April 20 and 26 (Fig. 16B, Table 4), but because it was not possible to measure every line every day, the exact timing of the changes cannot be determined. The two largest changes involve EC-1. Although it is possible that EDM set-up errors may have contributed to these, we do not consider this likely because the large changes involve initial line-length measurements made on two different days (EC-1 to EC-2 on 04/20/90 and EC-1 to EC-4 on 04/21/90). Instability of the ridge on which EC-1 was located is precluded by the minor changes measured in most lines over the 1-day period from 04/26/90 to 04/27/90.

Considering the April 1990 survey as a whole, the largest change was the +92 mm extension that took place between EC-4 and EC-1. This line has an azimuth of 340°, essentially across the shortest dimension of the caldera. The line from EC-5 to EC-4, which spans the northwest part of the caldera showed a contraction of 9 mm, although this is less than the 10 mm uncertainty in the data. The longest line, which runs approximately east–west between EC-5 and EC-3 also contracted, by 11 mm, barely above the data uncertainty. Between EC-1 and EC-2, a line with an azimuth of 95° along the southern rim of the caldera, 53 mm of extension took place. The line from EC-1 to EC-3, only 30° different from that between EC-1 and EC-2, however, showed barely detectable extension (14 mm).

The radial tilt arrays were established in Anatahan village (station NAMBO) and on the floor of the southeast crater (station SE_CRATER). Each consisted of two benchmarks 46.8 m apart along a line oriented approximately radial to the center of the island. No significant changes were measured along either tilt array during the 9-day study period.

12.2. Ground deformation measurements, June 1990

Reoccupation of the EDM network occurred on June 25 and 26, 1990. Essentially no line-length changes occurred since the April survey (Table 4). The only change above instrument uncertainty was 12 mm of extension along the line from EC-5 to EC-3,

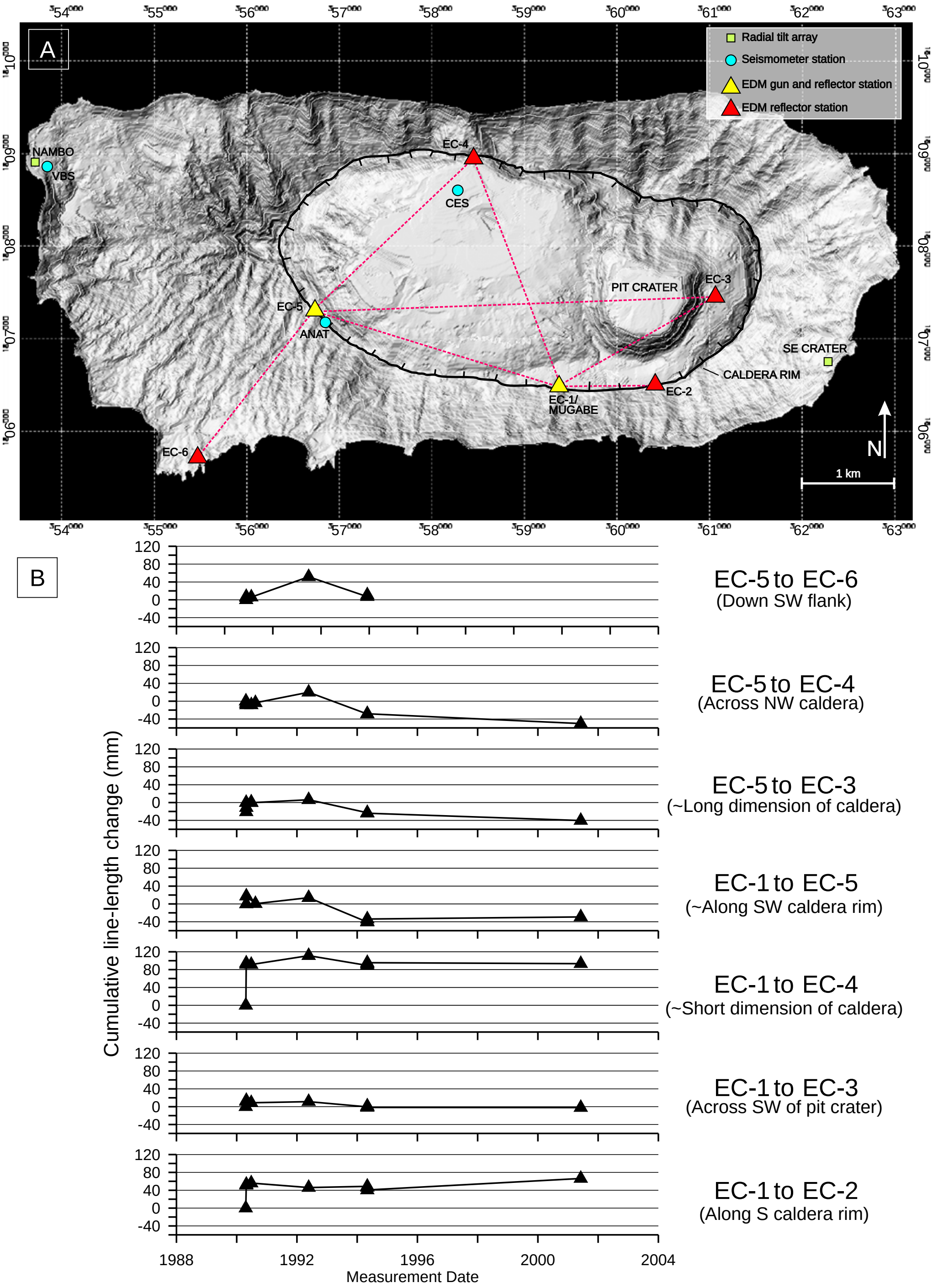

Fig. 16. A) Locations of geophysical monitoring stations (EDM shot points and reflectors, seismometer stations, and radial tilt arrays). B) Graphs of cumulative line-length changes for the Anatahan EDM network between April 1990 and June 2001 (positive = extension, negative = contraction). Note the distinct extension along some lines in April 1990, slight extension along most lines between 1990 and 1992, and gradual contraction along all lines except EC1 to EC2 from 1992 to 1994 and from 1994 to 2001.

Table 4

EDM mark-to-mark line-lengths (in m; no parentheses), change since previous measurement (in mm; parentheses), and cumulative change since first measurement (in mm; square brackets) at Anatahan, April 1990 to June 2001

EDM line	04/20/90	04/21/90	04/22/90	04/25/90	04/26/90	04/27/90	Total change in 04/90	06/25/90 or 06/26/90	10/01/90 or 10/04/90	05/22/92	05/03/94	06/04/01
EC-5 to EC-6	n.m.	n.m.	n.m.	2431.981	2431.988 (+7)	2431.986 (−2) [+5]	[+5]	2431.987 (+1) [+6]	n.m.	2432.033 **(+46)** [+52]	2431.992 **(−41)** [+11]	n.m.
EC-5 to EC-4	n.m.	n.m.	2442.111	2442.106 (−5)	2442.102 (−4) [−9]	n.m.	[−9]	2442.102 (0) [−9]	2442.097 (−5) [−14]	2442.131 **(+34)** [+20]	2442.082 **(−49)** [−29]	2442.060 **(−22)** [−49]
EC-5 to EC-3	n.m.	n.m.	n.m.	4310.747	4310.726 **(−21)**	4310.736 **(+10)** [−11]	**[−11]**	4310.748 **(+12)** [0]	n.m.	4310.754 (+7) [+7]	4310.723 **(−31)** [−24]	4310.707 **(−16)** [−40]
EC-1 to EC-5	n.m.	n.m.	n.m.	n.m.	2478.043	2478.060 **(+17)**	**[+17]**	n.m.	2478.039 **(−21)** [−4]	2478.057 **(+18)** [+14]	2478.003 **(−54)** [−40]	2478.013 **(+10)** [−30]
EC-1 to EC-4	n.m.	2562.984	n.m.	n.m.	2563.079 **(+95)**	2563.076 (−3) [+92]	**[+92]**	2563.075 (−1) [+91]	n.m.	2563.095 **(+20)** [+111]	2563.080 **(−15)** [+96]	2563.077 (−3) [+93]
EC-1 to EC-3	2091.096	n.m.	n.m.	n.m.	2091.108 **(+12)**	2091.110 (+2) [+14]	**[+14]**	2091.105 (−5) [+9]	n.m.	2091.107 (+2) [+11]	2091.097 **(−10)** [+1]	2091.094 (−3) [−2]
EC-1 to EC-2	1005.526	n.m.	n.m.	n.m.	1005.577 **(+51)**	1005.579 (+2) [+53]	**[+53]**	1005.582 (+3) [+56]	n.m.	1005.572 **(−10)** [+46]	1005.567 (−5) [+42]	1005.592 **(+25)** [+67]
EC-2 to EC-3	1456.202	n.m.	n.m.	n.m.	n.m.	n.m.	n.m.	n.m.	n.m.	n.m.	1456.196 (−6)	n.m.

Note that as of 05/03/94, MUGABE replaced EC-1; line lengths and changes have been adjusted for the station relocation. We used a Hewlett-Packard 3808A EDM gun, calibrated on National Geodetic Survey (NGS) lines in Hawai'i and Saipan. Temperature and pressure were measured only at the shot end of each EDM line. Station height was measured and all reflector heights were assigned a value of 50 cm. Signal strength was not optimal for the longest line (EC-5 to EC-3), and although lines were not shot 10 times during each survey, standard deviations of measurements are acceptable. Lack of temperature and pressure measurements at both ends of each line and reflector centering uncertainty lead to a measurement uncertainty of 10 mm. Bold face indicates change values greater than 10 mm. n.m. = not measured.

which spans most of the long dimension of the caldera (Fig. 16). This same line showed contraction by an equivalent amount during the April survey. The tilt arrays were not reoccupied.

12.3. Ground deformation measurements, October 1990

Only two lines were measured, because many reflectors were obscured by vegetation or filled with water. The line from EC-1 to EC-5, spanning the southwest part of the caldera, showed contraction of 21 mm. The line from EC-5 to EC-4, across the northwest part of the caldera, also contracted but by an amount less than the data uncertainty.

12.4. Ground deformation measurements, May 1992

Most of the EDM lines showed modest extension between 1990 and 1992 (Fig. 16B, Table 4). These include the north–south cross-caldera line (EC-1 to EC-4), which extended 20 mm, the line across the northwest part of the caldera (EC-5 to EC-4), which extended 34 mm, and the line extending down the southwest flank (EC-5 to EC-6), which extended 46 cm (Table 4). EC-1 to EC-5, which runs across the southwest part of the caldera extended 18 cm. The only line that contracted was EC-1 to EC-2, the line that runs parallel to the southeast part of the caldera rim. Thus, the overall extension was clearly concentrated in the western part of the caldera (Moore et al., 1993).

12.5. Ground deformation measurements, May 1994

Between May 1992 and May 1994, all the EDM lines contracted (Fig. 16B, Table 4). The greatest contraction occurred in the same region that had shown the greatest extension between 1990 and 1992, specifically the southwest–northeast-oriented lines connecting EC-6, EC-5, and EC-4. Contraction also occurred across the southwest part of the caldera (EC-1 to EC-5) as well as along the long axis of the caldera (EC-5 to EC-3). The smallest amounts of contraction occurred in the eastern and southeastern parts of the caldera. Again, the greatest amount of deformation was in the western part of the caldera (Sako et al., 1995).

12.6. Ground deformation measurements, June 2001

Line-length changes relative to those seen 7 years earlier were only moderate in 2001. Specifically, 22 cm of contraction occurred across the northwest part of the caldera (EC-5 to EC-4) and 16 mm of contraction occurred across the long east–west dimension (EC-5 to EC-3). The largest change was 25 mm of extension along the southeast caldera rim (EC-1 to EC-2; Fig. 16; Table 4).

12.7. Summary of ground deformation measurements

The greatest amount of EDM-measured deformation occurred during the April 1990 field visit. The deformation included large north–south extension across the caldera and east–west extension along the south caldera rim. Only minor extension occurred along the one line that crosses the pit crater. Simultaneously, the caldera as a whole contracted slightly along its long east–west dimension. The east–west contraction had reversed by June 1990 without other significant measured changes. The October 1990 data show only slight contraction across the southwest part of the caldera.

Most lines extended between 1990 (either June or October) and May 1992. This extension was most significant in the west and north parts of the caldera. In particular, two lines running roughly southwest–northeast, connecting EC-6, EC-5, and EC-4 (Fig. 16) lengthened. Overall extension of the west part of the caldera could achieve this. North–south extension was minimal, and, in the southeast part of the caldera, a small contraction occurred. Perhaps extension in the western part of the caldera caused a small amount of compression in the eastern part.

The overall extension between 1990 and 1992 was reversed between 1992 and 1994, some lines contracting to lengths less than their 1990 values. The behavior was essentially the opposite of the 1990–1992 extension, in that the contraction was greatest in the western part of the caldera and minimal in the eastern part.

The next measurements were made in June 2001. The contraction in the western caldera noted from 1992 to 1994 appears to have continued, although at a much lower rate averaged over the 7 years since the

1994 survey. The largest change noticed in 2001, both in magnitude and direction, was along the southeast caldera rim (EC-1 to EC-2). The lines that cross the pit crater, where the 2003 eruption was to occur less than 2 years later (EC-1 to EC-3 and EC-5 to EC-3), showed essentially no changes.

These EDM data cannot be explained by a simple homogeneous expansion of the volcano, because almost never was the activity all extension or all contraction. Different parts of the caldera rim were apparently able to move independently from one another as large blocks. Most of the largest extensions and contractions were measured in the western part of the caldera, which is somewhat unexpected given that the most vigorous geothermal activity (and the 2003 vent) are in the eastern part (Moore et al., 1993; Sako et al., 1995). The data are sparse, but suggest that the main magma chamber underlies the western part of the caldera. This in turn would imply that the conduit to the surface tilts to the east.

It is not possible to identify any clear indication of the coming 2003 eruption in the EDM data collected from 1990 to 2001.

12.8. Seismic investigations, April 1990

Upon arrival in Anatahan village, a seismic-monitoring station was set up in the schoolhouse (station VBS; Fig. 16) and run continuously for 9 days from April 19 to 27, 1990. This station consisted of a Kinematrics PS-2 portable seismograph and a 1 Hz Mark Products L4-C vertical-component seismometer. The instrument magnification was set at 24 and 18 dB (magnification at 1 Hz was roughly 4000 and 2000, respectively), and the low pass filter was set at 12.5 Hz. The seismometer location was relatively free of human-induced noise. Later in the monitoring period, surf noise began to swamp the seismic signal, necessitating reduction of the gain to 12 dB. Typical seismograms from station VBS are shown in Fig. 17A and B.

A second set of seismic measurements was made in the caldera (station CES; Fig. 16) using a strip-chart portable seismograph with a 1 Hz Mark Products L4-C vertical-component seismometer. Measurements were made at station CES only when helicopter transportation to the caldera was available, in particular 16:04–16:49 April 19, 06:57–08:03 April 20, 12:13–13:08 April 21, and 14:13–16:37 April 22.

Seismic surveillance indicated intermittent earthquakes local to the Anatahan region (i.e. beneath the island or within several tens of kilometers offshore; Table 5). None of the local earthquakes consisted of sustained swarms or tremor, and only one was felt. More distant earthquakes (200–300 km away) were also recorded. Both local and distant seismicity increased from April 19 to 23 and then decreased until April 27 (Fig. 17C; Table 5).

12.9. Seismic investigations, June 1990

Only station VBS was occupied during this brief (26 h) visit to the island. No local earthquakes with magnitudes >M2.5 were noticeable, suggesting a decrease in seismicity since April 1990. However, earthquake detection capability was reduced because significant surf noise (Fig. 17D) necessitated decreasing the gain to 12 dB during much of this visit.

12.10. Seismic investigations, October 1990

The major task of this 1-day visit to Anatahan was to install a permanent seismometer that would telemeter its data to the CNMI Civil Defense Headquarters on Saipan. The station would not only monitor Anatahan (Station ANAT) but also serve as a telemetry relay station for seismic data coming from stations set up a few days previously on Pagan and Alamagan. For this reason station ANAT was placed high on the southwest caldera rim (Fig. 16), with line-of-sight views to both Alamagan and Saipan. No significant shallow seismicity was recorded at this station during the first few months after its installation (Moore et al., 1991), and only 4 earthquakes were recorded in the vicinity of Anatahan by Station ANAT between October 1990 and February 1992.

12.11. Seismic investigations, May 1992

From May 13 to 15, 1992 a portable seismograph was operated on the caldera floor. No signals other than teleseisms and human-induced noise were recorded during these 2 days (Moore et al., 1993). Station ANAT was upgraded during the visit.

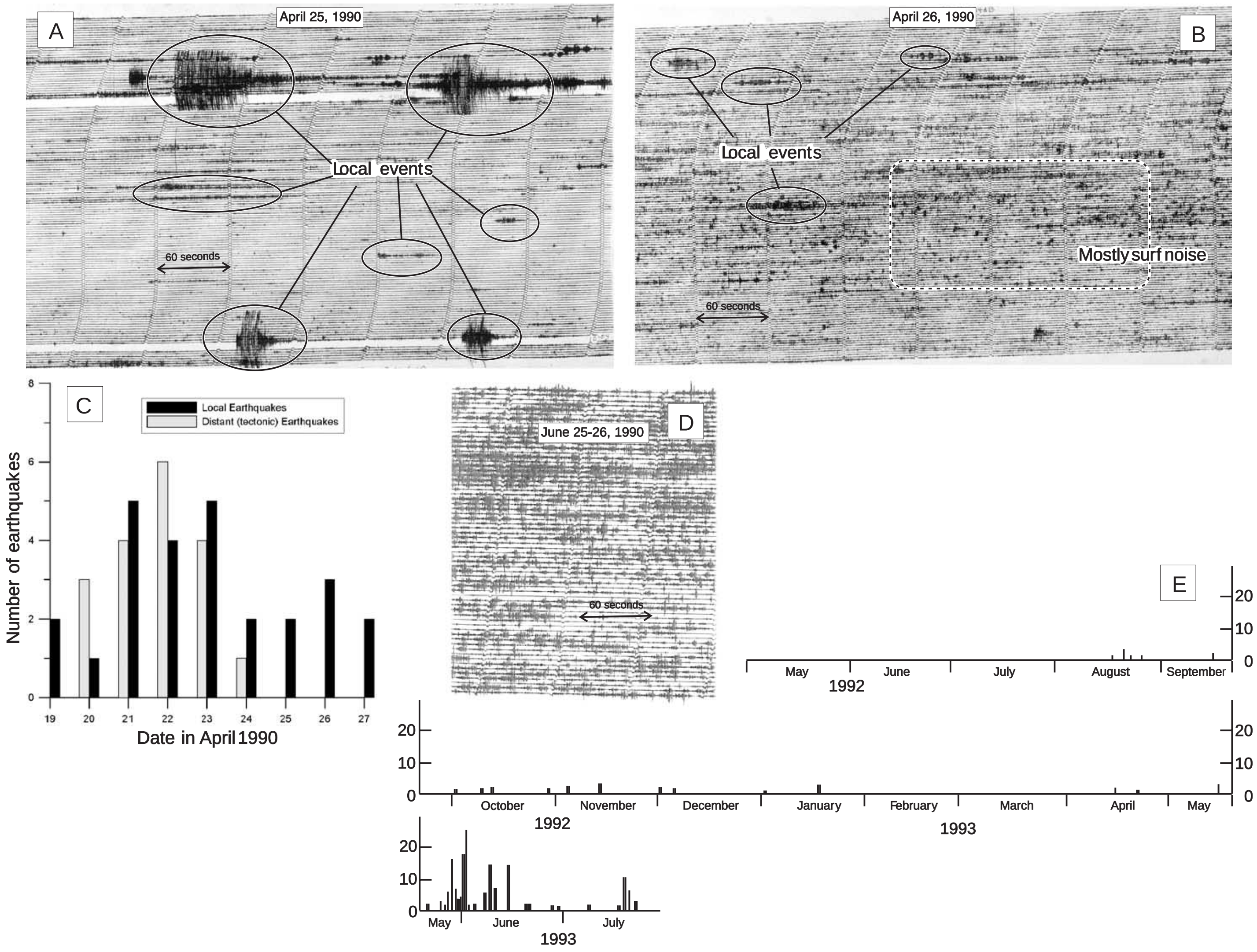

Fig. 17. Anatahan seismic data and observations. A) Sample record from station VBS prior to increase in ocean surf. Interval covers 07:33:09 April 25, 1990 until 07:10:40 April 26, 1990 (times are local). B) Sample record from station VBS after increase in ocean surf. Interval covers 07:55:46 April 26, 1990 until 07:12:15 April 27, 1990 (times are local). C) Earthquakes identified between April 19 and 27, 1990 (Table 5). D) Portion of seismic record from the night of June 25–26, 1990. Heavy surf noise necessitated setting the instrument to a lower magnification. E) Daily number of local earthquakes (S-P < 5 s) recorded at seismic station ANAT from August 1992 to July 1993. Data from ANAT are telemetered to, and recorded at, the CNMI Emergency Management Office on Saipan.

Table 5
List of earthquakes recorded at Anatahan, April 19–27, 1990

Date	Local time (hh:mm:ss)	Approx. distance from station (km)	Approx. magnitude from signal duration
April 19	22:57:12	5	1.7
	23:37:28	30	2.2
April 20	01:49:36	270	2.9
	01:59:58	270	2.9
	18:17:03	250	3.5
	19:51:02	35	1.3
April 21	04:41:31	35	3.2 (felt mildly)
	04:49:00	30	1.8
	08:40:50	30	0.8
	11:27:35	250	4.7
	15:01:39	10	0.4
	18:48:28	20	1.6
	19:01:16	270	4.0
	20:56:28	270	3.0
	21:06:05	250	3.4
April 22	01:50:13	30	1.6
	10:31:33	35	1.8
	10:37:22	250	3.6
	10:49:28	240	3.7
	11:44:49	250	3.5
	11:56:43	250	4.2
	12:01:20	240	3.5
	14:41:22	25	0.7
	14:42:40	30	1.7
	20:32:43	280	3.1
April 23	00:07:52	280	3.7
	00:22:51	280	3.5
	05:02:19	270	3.7
	17:22:51	25	3.2
	18:04:23	35	3.5
	18:06:45	40	2.3
	21:46:22	58	2.2
	23:30:00	250	3.5
April 24	04:57:35	30	0.5
	10:03:04	55	2.0
	14:55:53	280	3.9
April 25	11:47:22	30	1.5
	12:08:00	35	4.5
April 26	05:59:14	35	2.7
	06:02:17	35	2.2
	17:53:10	38	1.5
April 27	05:38:34	10	0.8
	12:11:37	10	1.0
	13:06:35	10	1.0

12.12. Seismic investigations, May 1994

Data were only intermittently available from Station ANAT between 1992 and 1994. Nine earthquakes > M4.5 were recorded in the Anatahan vicinity between late 1992 and May of 1994 (Sako et al., 1995), and swarms of small, local, earthquakes took place from May to July 1993 (Fig. 17E).

12.13. Seismic investigations, June 2001

No field seismograph was deployed during the June, 2001 visit. Although station ANAT was working until 2001, the telemetry equipment on Saipan failed in August, 1999. Instead of simultaneously recording data from all the Northern Mariana seismic stations (2 on Pagan and 1 each on Alamagan and Anatahan), only one station could be monitored at a time. Most attention was paid to Pagan. During the times that the equipment was set to record seismicity from station ANAT, no earthquakes were recorded. The National Earthquake Information Center (NEIC) catalog of regional earthquakes > M4 showed no concentration in the Anatahan area occurred in the interval from May 1994 to June 2001.

12.14. Summary of Anatahan seismicity, April 1990–June 2001

Most locally generated seismicity was associated with the March–April 1990 crisis. Since then, only the few minor swarms in May–July 1993 can be considered to be elevated activity. As with the EDM results, there were no obvious seismic precursors recorded prior to the 2003 eruption. However, seismic data were collected only infrequently. The permanent station ANAT and the telemetry equipment on Saipan were unreliable during much of the time considered by this report, so that the seismic record is largely blank. The situation did not improve between the June 2001 visit and the May 2003 eruption.

13. Recommendations made after field visits

Following each field visit, recommendations were made to the CNMI Civil Defense office (now called the Emergency Management Office; EMO). We were careful to make these recommendations only to the EMO. Decisions regarding Anatahan residents, and statements to the press about these decisions, were made by EMO spokespeople rather than by the geologists.

Based on the geological and geophysical observations in April 1990, the following recommendations were made (Koyanagi et al., 1990): (1) Do not send the residents back unless a seismometer is installed on Anatahan. (2) Re-occupy the EDM network in a few months to determine if line-length changes were continuing. (3) Arrange for someone from the CNMI EMO to enroll in the Center for the Study of Active Volcanoes (CSAV) course at the University of Hawai'i at Hilo. In response to this, a seismometer was purchased but set up on Saipan rather than Anatahan. Two CNMI EMO personnel took the CSAV course in the summer of 1990.

After the June 1990 visit, the recommendations were essentially the same (Sako et al., 1990): (1) Do not send the residents back unless a seismometer is installed on Anatahan. (2) Regular aerial observations of the island should be scheduled regardless of whether or not the residents return. (3) The EDM network should be re-occupied if another seismic swarm occurs, if overflights note changes in activity within the pit crater or elsewhere, if other work such as installing a permanent seismometer will take trained personnel to the island, or within a year if none of these events occurs. By this time plans had been made to establish a telemetered seismic network on a number of the northern CNMI islands, including Anatahan.

After the October 1990 visit, during which the permanent seismic network was established, the recommendations were to maintain and strengthen the seismic stations and, importantly, to continue the efforts to train local CNMI staff to upkeep the equipment and assess the data (Moore et al., 1991). Similar recommendations were made after the May 1992 visit, except that they were more explicit. Specifically, a portable seismic station should be maintained on each inhabited island (Agrigan, Alamagan, Anatahan, and (intermittently) Pagan), and a resident of each island should be trained to read the seismic records (Moore et al., 1993). If increased or unusual seismic activity is detected by the portable seismometer, the trained person will radio the CNMI EMO on Saipan for advice and more careful assessment of the data. The effort to install this equipment would also offer the opportunity to educate the local population about natural hazards. This is critical, because in addition to volcanic hazards, close proximity of all the islands to the large-earthquake-generating Mariana subduction zone poses a severe tsunami risk.

Unofficial re-settlement of Anatahan began sometime before the May 1994 visit. After the visit, the recommendation to install portable seismometers on populated islands was repeated, and it was also suggested that residents keep a log of seismic activity to be archived and sent to CNMI EMO for analysis. Because of concerns about upkeep of the permanent seismic network, urgent recommendations were made to repair the equipment whenever necessary (Sako et al., 1995). The recommendation that local CNMI residents become trained in volcano monitoring was also repeated, and during the next few years, 5 CNMI EMO staff completed the CSAV course. After the June 2001 visit, essentially the same recommendations as those issued after the May 1994 visit were repeated (Trusdell et al., 2001). These were particularly important because at the time, the CNMI government was developing a plan to resettle Anatahan, Agrigan, and Alamagan, and to allow short visits to Pagan.

14. Conclusions

We presented reconnaissance geologic observations and a chronology of intermittent observations and geophysical data for an 11-year period (1990 to 2001). The overall geology and structure of Anatahan is typical for an island stratovolcano, namely intercalated lava flows and ash deposits producing a cone with slopes of 30–40°. A caldera truncates the cone, and activity subsequent to caldera formation partially filled the caldera. A pit crater in the eastern part of the caldera has been the location of geothermal activity since at least the 1940s and is the locus of current eruptive activity. The elongate shape of Anatahan is somewhat unusual and suggests coalescence of two volcanoes, but we could find no strong evidence for this idea. The caldera, on the other hand, is clearly compound, produced by the coalescence of eastern and western collapse structures. The straight north and south coastlines are perhaps related to large-scale mass-wasting, but other geologic evidence for this is scarce.

We qualitatively divided the stratigraphy into 3 stages. Stage 1 consists of the bulk of the island and includes all the pre-caldera units. Stage 2 is considered post-caldera, including units that partially fill the caldera as well as vents and flows on the outer flanks that are young enough to be morphologically identifiable. Stage 3 is a young (few hundred years old) hydromagmatic unit that covers much of the island. It probably was produced by activity similar to that in 2003. Other, similar, ash units underlie the stage 3 ash exposed in the upper walls of the pit crater. Their presence bears on where we consider the May 2003 eruption to fit into the Anatahan history. It may be most accurate to define stage 3 as a period of intermittent (i.e. every few hundred years) hydromagmatic activity owing to the presence of the pit crater and to include the current eruption as part of this stage.

A seismic crisis in the spring of 1990 prompted our first visit and led eventually to the installation of a permanent seismometer on the island. Unfortunately, geophysical and geological monitoring has been infrequent since then, and no clear patterns of geothermal activity, deformation, or seismicity can be identified. Geothermal activity in pits within the pit crater was relatively stable over the observation period, at least as far as the infrequent observations are concerned. On the whole, water levels within the pits decreased during the 11-year observation period, but which pits were or were not active changed little. Only during the June 2001 visit was there an apparent increase in the area of geothermal activity around a couple of the pits, but it was not dramatic. The shallow lake proved problematic with respect to changes in activity. The lake water is meteoric and therefore tends to be clear, but its appearance changes significantly depending on whether or not the lake extends far enough to incorporate one or more of the sediment-laden active pits. When this occurs, the pH of the lake water decreases and vegetation is killed. Noticing (e.g. from an overflight) that the lake water is cloudy and that vegetation has died may be more an observation of recent heavy rains than of a change in volcanic activity.

Geodetic data likewise are difficult to use to identify patterns, particularly any that would have presaged the 2003 eruption. The overall pattern was one of extension during April 1990 followed by slow contraction up to 2001. Most of the line-length changes (both extension and contraction) occurred in the western part of the caldera, not near the active geothermal area in the pit crater. Seismicity also apparently peaked during the spring of 1990, although it was only during that first field visit that more than 2 days of monitoring occurred. The permanent seismometer and its telemetering system were plagued with equipment failures and provided only an intermittent record of earthquake activity. The geological teams continually encouraged CNMI EMO to keep the equipment in good working order and to train and educate the local Anatahan population with respect to geological hazards.

Acknowledgements

We thank the people of Anatahan and Saipan for their hard work and assistance, and for making our stays on Anatahan enjoyable. CNMI Governors Larry Guerrero, Froilan Tenorio, and Pedro Tenorio, EMO Directors Felix Sasamoto, Francisco Chong, and Greg DeLeon Guerrero, and Northern Islands Mayors Valentin Taisakan, Joseph Ogumoro and Ambrosio Ruben all provided considerable logistical assistance, as did Dept. of Public Safety officer Mike Camacho and Fire Division Medic Donald Taitano. We acknowledge the hardworking staff of CNMI EMO, including Ben Lieto, Joe Basa, Mark Pangelinan, Juan Takai Camacho, Tony Tenorio, Joe Kaipat, Tom Crisostomo, Charlie Klakidm, Paul Cruz, Joe Basa, and Mark Pangelinan, as well as seismic technicians Ramon Chong and Ignacio Borja. Helicopter pilots of U.S. Navy Squadron HC-5 (A. Worley, Commander), Pacific Islands Aviation (T. Allan), and Americopters (Rufus Crowe and Mike Cunningham) provided excellent support; without their efforts the geophysical network could not have been installed or revisited. John Hoffmann as well as the captain and crew of the “Stella” assisted with field observations, and Harold Garbeil helped produce the DEM used for Figs. 2 and 16. Michele Tuttle analyzed the water samples and, along with Don Thomas, helped with understanding them. Dave Siems, James Budahn, T. Peacock, and J. Mee analyzed the rock samples. Reviews by Don Swanson and Robert Stern improved the manuscript. This is HIGP paper 1350 and SOEST contribution no. 6473.

References

Banks, N.G., Koyanagi, R.Y., Sinton, J.M., Honma, K.T., 1984. The eruption of Mount Pagan volcano, Mariana Islands, 15 May 1981. J. Volcanol. Geotherm. Res. 22, 225–270.

BGVN, 1990a. Bulletin of the Global Volcanism Network for March 1990, 15, no. 3, 8–9.

BGVN, 1990b. Bulletin of the Global Volcanism Network for April 1990, 15, no. 4, 13–14.

BGVN, 1990c. Bulletin of the Global Volcanism Network for June 1990, 15, no. 6, 8.

BGVN, 1990d. Bulletin of the Global Volcanism Network for September 1990, 15, no. 9, 9.

BGVN, 1990e. Bulletin of the Global Volcanism Network for October 1990, 15, no. 10, 7.

BGVN, 1992. Bulletin of the Global Volcanism Network for June 1992, 17 no. 6, 7.

BGVN, 1994. Bulletin of the Global Volcanism Network for February 1994, 19, no. 2, 3–5.

BGVN, 1995. Bulletin of the Global Volcanism Network for October 1995, 20, no. 10, 12–13.

BGVN, 1999. Bulletin of the Global Volcanism Network for January 1999, 24, no. 1, 8.

BGVN, 2001. Bulletin of the Global Volcanism Network for May 2001, 26, no. 5, 8–9.

BGVN, 2003a. Bulletin of the Global Volcanism Network for April 2003, 28, no. 4, 2–3.

BGVN, 2003b. Bulletin of the Global Volcanism Network for May 2003, 28, no. 5, 2-2-5.

BGVN, 2003c. Bulletin of the Global Volcanism Network for June 2003, 28, no. 6, 10–11.

BGVN, 2003d. Bulletin of the Global Volcanism Network for July 2003, 28, no. 7, 2–3.

BGVN, 2003e. Bulletin of the Global Volcanism Network for September 2003, 28, no. 9, 4.

BGVN, 2004. Bulletin of the Global Volcanism Network for April 2004, 29, no. 4, 7–8.

Bloomer, S.H., Stern, R.J., Smoot, N.C., 1989. Physical volcanology of the submarine Mariana and Volcano arcs. Bull. Volcanol. 51, 210–224.

Chadwick, W.W. Jr., Embley, R.W., Johnson, P.D., Merle, S.G., Ristau, S., Bobbitt, A., 2005. The submarine flanks of Anatahan Volcano, commonwealth of the Northern Mariana Islands. J. Volcanol. Geotherm. Res. 146, 8–25 (this issue).

Cloud, P.E., Schmidt Jr., R.G., Burke, H.W., 1956. Geology of Saipan Mariana Islands. U.S. Geol. Surv. Prof. Pap. 280-A, 155 pp.

Corwin, G., 1971. Quaternary volcanics of the Marianas Islands. Unpublished ms, 137 pp.

Cox, K.G., Bell, J.D., Pankhurst, R.J., 1979. The Interpretation of Igneous Rocks. George Allen & Unwin, London, 450 pp.

Driver, M.G., 1992. History of the Marianas, Caroline, and Palau Islands. English transl. of: Ibáñez y García, L. 1887. Historia de las Islas Marianas, con su derrotero, y de Carolinas y Palaos, desde el Descburimiento por Magallanes en el año 1521, hasta nuestros días. Micronesian Area Research Center, Univ. Guam, 193 pp.

Embly, R.W., Baker, E.T., Chadwick, W.W., Lupton, J.E., Resing, J.A, Massoth, G.J., Nakamura, K., 2004. Explorations of Mariana Arc volcanoes reveal new hydrothermal systems. EOS, Trans.-Am. Geophys. Union 85 (4), 37–44.

Fairbridge, R.W., 1950. Landslide patterns on oceanic volcanoes and atolls. Geogr. J. 115, 84–88.

Fryer, P., 1996. Evolution of the Mariana convergent plate margin system. Rev. Geophys. 34, 89–125.

Gorshkov, A.P., Gavrilenko, G.M., Seliverstov, N.I., Scripko, K.A., 1982. Geologic structure and fumarolic activity of the Esmeralda submarine volcano. In: Schmincke Jr., H.-U., Baker, P.E., Forjaz, V.H. (Eds.), Proc. Symp. Activity Oceanic Volcanoes, Arquipelago, vol. 3. Revista Univ. Dos Acores, pp. 271–298.

Karig, D.E., 1971. Structural history of the Mariana island arc system. Geol. Soc. Am. Bull. 82, 323–344.

Koyanagi, R., Kojima, G., Lockwood, J., Sako, M., Rowland, S. 1990. “Revised” preliminary report of the Anatahan volcanic crisis investigation team on the 19–27 April, 1990 visit to Anatahan. Report prepared for the Office of Civil Defense, CNMI June 6, 1990, 18 pp.

Koyanagi, R., Kojima, G., Chong, F., Chong, R. 1993. Seismic monitoring of earthquakes and volcanoes in the Northern Mariana Islands: 1993 summary report: Prepared for the Office of the Governor, CNMI, February 21, 1993, 34 pp.

Kuno, H., 1962. Japan, Taiwan and Marianas. Catalog of active volcanoes of the world and solfatara fields, Rome. IAVCEI 11, 1–332.

Lambeck, K., 2004. Sea-level change through the last glacial cycle: geophysical, glaciological and paleogeographic consequences. C. R. Geosci. 336, 677–689.

Maruyama, M., 1954. Anatahan. Weidenfeld and Nicolson, London, 191 pp.

McClelland, L., Simkin, T., Summers, M., Nielsen, E., Stein, T.C., 1989. Global Volcanism 1975–1985. Prentice Hall, Englewood Cliffs, NJ, 655 pp.

Meijer, A., Reagan, M., Ellis, H., Shafigullah, M., Sulter, J., Damon, P., Kling, S., 1983. Chronology of volcanic events in the eastern Philippine Sea: Part 2. Am. Geophys. Union Geophys. Monogr. 27, 349–359.

Moore, R.B., Trusdell, F.A., 1993. Geologic map of Alamagan Volcano, Northern Mariana Islands. U.S. Geol. Surv. Map I-2408.

Moore, R.B., Koyanagi, R.Y., Sako, M.K., Trusdell, F.A., Kojima, G., Ellorda, R., Zane, S. 1991. Volcanologic Investigations in the Commonwealth of the Northern Mariana Islands, September–October 1990. U.S. Geol. Surv. Open-File Rpt. 91-320, 31 pp.

Moore, R.B., Koyanagi, R.Y., Sako, M.K., Trusdell, F.A., Ellorda, R.L., Kojima, G, 1993. Volcanologic Investigations in the Commonwealth of the Northern Mariana Islands, May 1992. U.S. Geol. Surv. Open-File Rpt. 93-541, 37 pp.

Nakada, S., Matsushima, T., Yoshimoto, M., Sugimoto, T., Kato, T., Watanabe, T., Chong, R., Camacho, J.T., 2005. Geological aspects of the 20032004 eruption of Anatahan Volcano, Northern Mariana Islands. J. Volcanol. Geotherm. Res. 146, 226–240 (this issue).

Norris, R.A., Johnson, R.H., 1969. Submarine volcanic eruptions recently located in the Pacific by SOFAR hydrophones. J. Geophys. Res. 74, 650–664.

Pallister, J.S., Trusdell, F.A., Brownfield, I.K., Siems, D.F., Budahn, J.R., Sutley, S.F., 2005. The 2003 phreatomagmatic eruptions of Anatahan Volcano—textural and petrologic features of deposits at an emergent island volcano. J. Volcanol. Geotherm. Res. 146, 208–225 (this issue).

Sako, M., Koyanagi, R., Rowland, S. 1990. “Revised” preliminary report of the second visit to Anatahan, CNMI by the U. S. Geological Survey Hawaiian Volcano Observatory “Anatahan Crisis Team”, June 25–26, 1990. Rept. prepared for the Office of Civil Defense, CNMI, July 6, 1990, 8 pp.

Sako, M.K., Trusdell, F.A., Koyanagi, R.Y., Kojima, G., Moore, R.B. 1995. Volcanic investigations in the Commonwealth of the Northern Mariana Islands. April to May 1994. U.S. Geol. Surv. Open-File Rpt. 94-705, 57 pp.

SEAN, 1987. Scientific Event Alert Network Bulletin for August 1987. 12, no. 8.

Siebert, L., 1984. Large volcanic debris avalanches; characteristics of source areas, deposits, and associated eruptions. J. Volcanol. Geotherm. Res. 22, 163–197.

Siebert, L., Glicken, H., Ui, T., 1987. Volcanic hazards from Bezymianny- and Bandai-type eruptions. Bull. Volcanol. 49, 435–449.

Simkin, T., Siebert, L., 1994. Volcanoes of the World. Geoscience Press, Tucson, 349 pp.

Stearns, H.T., 1978. Quaternary shorelines in the Hawaiian islands. Bernice P. Bishop Mus. Bull. 237, 57 pp.

Stern, R.J., Fouch, M.J., Klemperer, S.L., 2003. An overview of the Izu–Bonin–Mariana subduction factory. Geophys. Monogr. 138, 175–222.

Tanakadate, H., 1940. Volcanoes in the Mariana Islands in the Japanese Mandated South Seas. Bull. Volcanol. 6, 199–225.

Trusdell, F.A., Sako, M.K., Moore, R.B., Koyanagi, R.Y., Schilling, S., 2001. Preliminary studies of seismicity, ground deformation, and geology, Commonwealth of the Northern Mariana Islands, May 20 to June 8, 2001. Report prepared for Office of the Governor, CMNI, http://www.cnmiemo.org/Preliminary%20Studies%20Northern%20Mariana%20Islands.htm.

Trusdell, F.A., Moore, R.B., Sako, M., White, R.A., Koyanagi, S.K., Chong, R., Camacho, J.T., 2005. The 2003 eruption of Anatahan Volcano, Commonwealth of the Northern Mariana Islands: chronology, volcanology, and deformation. J. Volcanol. Geotherm. Res. 146, 184–207 (this issue).

Varekamp, J.C., Kreulen, R., 2000. The stable isotope geochemistry of volcanic lakes, with examples from Indonesia. J. Volcanol. Geotherm. Res. 97, 309–327.

Wade, J.A., Plank, T., Stern, R.J., Tollstrup, D.L., Gill, J.B., O’Leary, J.C., Eiler, J.M., Moore, R.B., Woodhead, J.D., Trusdell, F., Fischer, T.P., Hilton, D.R., 2005. The May 2003 eruption of Anatahan volcano, Mariana Islands: geochemical evolution of a silicic island-arc volcano. J. Volcanol. Geotherm. Res. 146, 139–170 (this issue).